Int J Earth Sci (Geol Rundsch) (2002) 91:594–614
DOI 10.1007/s00531-001-0243-x

ORIGINAL PAPER

Ralf Schmidt · Hans-Ulrich Schmincke

From seamount to oceanic island, Porto Santo, central East-Atlantic

Received: 21 February 2001 / Accepted: 25 October 2001 / Published online: 21 June 2002

Abstract The uplifted and deeply eroded volcanic succession of Porto Santo (central East-Atlantic) is the product of a wide spectrum of dynamic processes that are active in shoaling to emergent seamounts. Two superimposed lapilli cones marking the base of the exposed section are interpreted as having formed from numerous submarine to subaerial phreatomagmatic explosions, pyroclastic fragmentation being subordinate. The lower basaltic and the upper mugearitic to trachytic sections are dominated by redeposited tephra and are called 'lapilli cone aprons'. Vertical growth due to accumulation of tephra, voluminous intrusions, and minor pillowed lava flows produced ephemeral islands which were subsequently leveled by wave erosion, as shown by conglomerate beds. Periods of volcanic quiescence are represented by abundant biocalcarenite lenses at several stratigraphic levels. The loose tephra piles became stabilized by widespread syn-volcanic intrusions such as dikes and trachytic to rhyolitic domes welding the volcanic and volcaniclastic ensemble into a solid edifice. Shattering of a submarine extrusive trachytic dome by pyroclastic and phreatomagmatic explosions, accentuated by quench fragmentation, resulted in pumice- and crystal-rich deposits emplaced in a prominent submarine erosional channel. The dome must have produced an island as indicated by a collapse breccia comprising surf-rounded boulders of dome material. Subaerial explosive activity is represented by scoria cones and tuff cones. Basaltic lava flows built a resistant cap that protected the island from wave erosion. Some lava flows entered the sea and formed two distinct types of lava delta:

1. closely-packed pillow lava and massive tabular lava flows along the southwestern coast of Porto Santo, and
2. a steeply inclined pillow-hyaloclastite breccia prism composed of foreset-bedded hydroclastic breccia, variably-shaped pillows, and thin sheet flows capped by subhorizontal submarine to subaerial lava flows along the eastern coast of Porto Santo.

The facies architectures indicate emplacement:

1. on a gently sloping platform in southwestern Porto Santo, and
2. on steep offshore slopes along high energy shorelines in eastern Porto Santo.

Growth of the pillow-hyaloclastite breccia prism is dominated by the formation of foreset beds but various types of syn-volcanic intrusions contributed significantly. Submarine flank eruptions occurred in very shallow water on the flanks of the hyaloclastite prism in eastern Porto Santo. The island became consolidated by intrusion of numerous dikes and by emplacement of prominent intrusions that penetrate the entire volcanic succession. Volcanic sedimentation ended with the emplacement of a debris avalanche that postdates the last subaerial volcanic activity.

Keywords Eastern Atlantic · Madeira archipelago · Shoaling oceanic island · Seamount · Submarine volcanism · Volcanic processes · Tuff cone · Felsic dome · Lava delta

R. Schmidt · H.-U. Schmincke (✉)
GEOMAR Forschungszentrum, Wischhofstr. 1–3, 24148 Kiel, Germany
e-mail: hschmincke@geomar.de

Introduction

In July 1831, a small volcanic islet was born in the Mediterranean Sea about halfway between Sicily and Pantelleria. It was immediately claimed by several European powers because of the strategically important gateway to the eastern Mediterranean. The British name Graham Island is most commonly used, although it is also known as Ferdinanda in Italy. The tephra cone had reached its maximum dimensions of almost 0.5 km in diameter and about 60 m in height after the climax of volcanic activity in the middle of August. The loose tephra pile was quickly eroded by wave action and after only three months, the island was almost leveled and finally disappeared by January 1832 (Poulet Scrope 1862; Francis 1995). This sce-

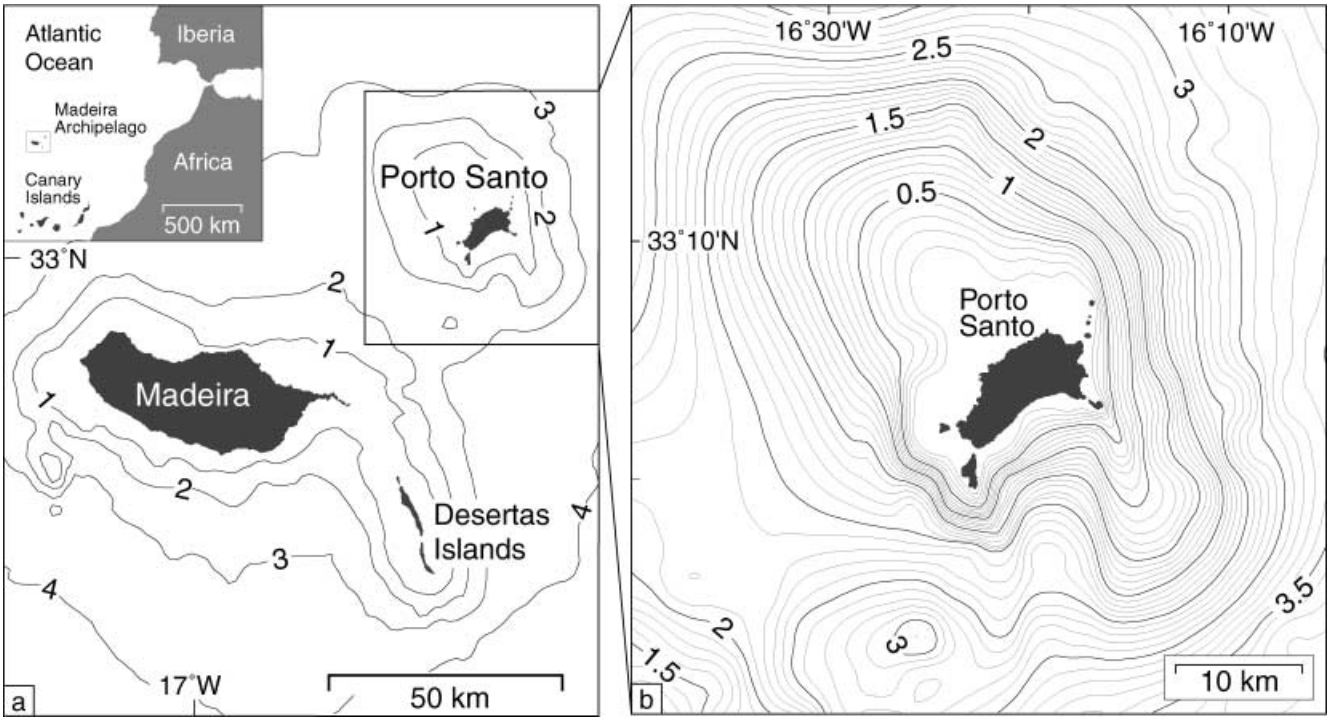

Fig. 1 **a** Madeira island group, contour interval 1 km. *Inset* shows the Madeira archipelago in the central eastern Atlantic. **b** Bathymetry of the vicinity of Porto Santo. Contour interval is 0.1 km. Data from the TOPEX data set (Smith and Sandwell 1997)

nario illustrates the normal fate of emergent seamounts trying to establish themselves as a volcanic island.

Little is known about the volcanic processes of shoaling to emergent seamounts, because deposits of this stage transitional in the growth of volcanic ocean islands commonly lie far below sea level, owing to subsidence of the islands grown on oceanic lithosphere (Watts and ten Brink 1989). Studies of modern marine shoaling to emergent volcanoes, e.g. Surtsey (Iceland), Myojinsho (Japan), and Metis Shoal (Tonga Islands), and of numerous seamounts, are commonly based on the interpretation of surface topography and limited sampling using submersibles (Lonsdale and Batiza 1980), bathymetric data (Fornari et al. 1984), dredging (Moore and Fiske 1969), drill-hole data (Fleet and McKelvey 1978), and on observations of the succession of events that occurred during eruptions (Kokelaar 1983; Moore 1985; Fiske et al. 1998). The internal structure of seamounts, however, remains poorly known.

Uplifted and dissected deep-water to shoaling volcanoes (Staudigel and Schmincke 1984; Schmincke and Bednarz 1990; Kano et al. 1993; McPhie 1995) provide insights into the internal structure of seamounts. Such sections generally lack the transitional (shoaling to emergent) stage, however, because this stage is small in volume compared with the entire edifice and is easily eroded by wave action (Schmidt and Schmincke 2000). The uplifted Tok Islands (Korea) are, as far as we are aware, the only example of a shoaling to emergent island volcano located in a marine setting in which the transitional stage is preserved (Sohn 1995). Several lacustrine englacial successions reveal the internal structure of shoaling to emergent volcanoes particularly well (Smellie and Hole 1997; Werner and Schmincke 1999), because wave energy in restricted basins is low compared with those in open marine environments and sudden drainage of glacial lakes can result in abrupt transition from subaqueous to subaerial conditions. Studies of uplifted submarine shoaling volcanoes and their englacial counterparts have led to a general model of seamounts growing above sea level to form an island. Volcanoes start in deep water with effusive pillow lava-sheet flow complexes intruded by dikes and sills with minor intercalated hyaloclastites (Schmincke and Bednarz 1990). Although vesiculation and explosive fragmentation of volatile-rich magmas can start at water depths exceeding 1,000 m (Gill et al. 1990; Clague et al. 2000), the amounts of clastic material and clast vesicularity generally increase during shoaling and culminate in shallow-water to emergent explosive tuff cones (Sohn and Chough 1992). The subaerial stage typically produces subhorizontal lava flows and associated lava deltas that originate from lava flows that enter the sea (Jones and Nelson 1970; Moore et al. 1973; Peterson 1976; Porebski and Gradzinski 1990; Schmincke et al. 1997). Mass wasting processes accompany all growth stages (Schmidt and Schmincke 2000).

Here we focus on the constructive and destructive volcanic and sedimentary processes that occur in shallow-water to emergent volcanoes. Porto Santo (Madeira Archipelago, central East-Atlantic) offers the unique opportunity to study this transitional stage of volcanic ocean island evolution in its complexity owing to uplift of this Miocene island and its subsequent erosion.

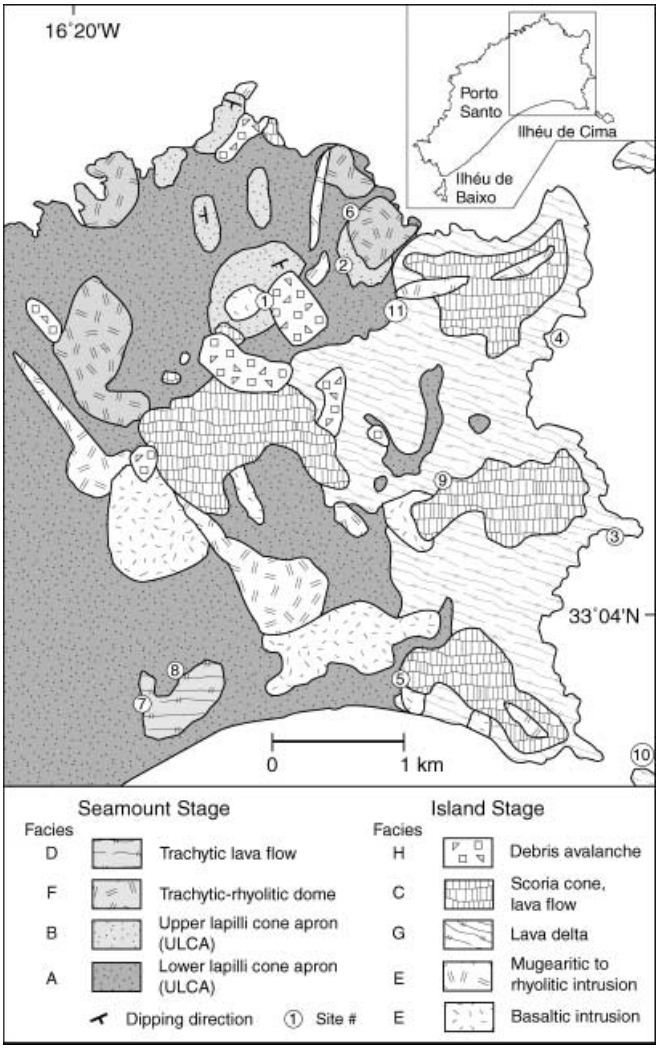

Fig. 2 Simplified geological map of eastern Porto Santo. Based on reconnaissance work by HUS and later studies by Jocelyn McPhie and RS

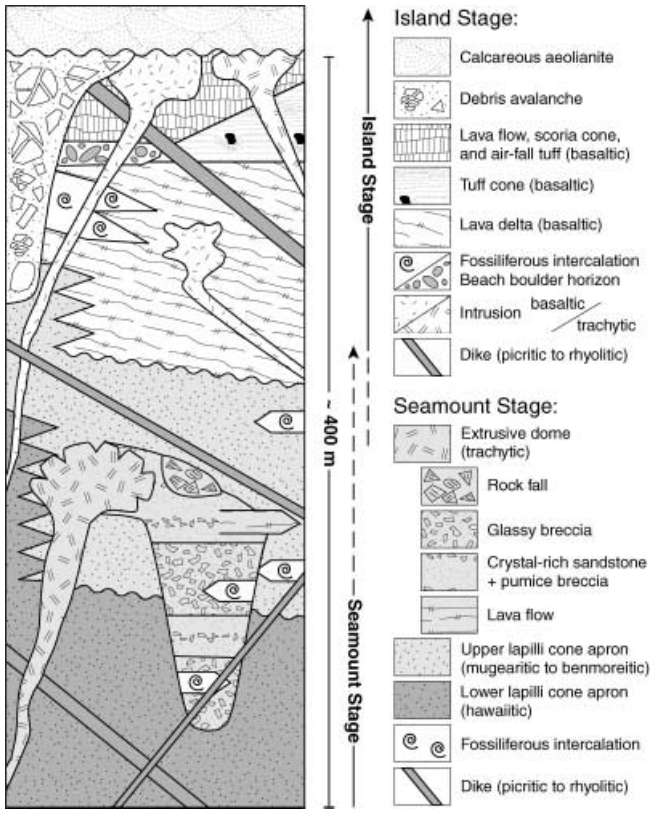

Fig. 3 Generalized stratigraphic section of Porto Santo. The extrusive dome, part of the Seamount Stage, is schematically illustrated to represent numerous trachytic to rhyolitic domes

Porto Santo

Porto Santo is located ca. 700 km off NW-Africa (Fig. 1a). Bathymetry shows that the island represents the partly eroded subaerial portion of a much larger submerged edifice (ca. 80 km×40 km) that rises from water depths of more than 3,000 m. The edifice has a flat top at ca. 100 m below sea level (b.s.l) and is star-shaped in plan view with a prominent NW–SE oriented rift zone (Fig. 1b). Volcanic rocks comprise dominantly alkali basalts, with minor mugearites, benmoreites, trachytes, and rhyolites (Schmincke and Weibel 1972). Most rocks exposed on the island are submarine in origin. The submarine series can be divided into an older, trachytic series (intrusions, flows, and related hyaloclastites) unconformably overlain by a basaltic-hawaiitic submarine to subaerial series (pillow lavas, associated hyaloclastite breccias, and intercalated fossil-bearing calcarenites grading into subaerial lava flows towards the top of the section). Submarine rocks occur at least as high as 300 m above sea level, indicative of uplift of the island, lowering of sea level, or both (Schmincke and Staudigel 1976; Feraud et al. 1981). Fossiliferous limestones intercalated with volcanic deposits are of mid-Miocene (ca. 14 Ma) age (Lietz and Schwarzbach 1970; Rodrigues et al. 1998). K/Ar ages indicate that most of the exposed volcanic rocks were emplaced between 12.5 and 13.8 Ma (Macedo et al. 1974; Feraud et al. 1981). Our new age data from subaerially exposed rocks of Porto Santo, discussed more fully elsewhere, indicate that this part of the volcano was formed between ca. 14 and 10 Ma (see also Geldmacher et al.; 2000). First emergence of the volcano occurred around 14 Ma, whereas younger rocks are subaerially erupted and submarine and/or subaerially emplaced. A simplified geological map of eastern Porto Santo and a generalized stratigraphic section are given in Figs. 2 and 3.

Deposits resulting from explosive processes

Submarine lapilli cone aprons

Two submarine to subaerially formed hydroclastic tephra cones form the base of the succession exposed in eastern Porto Santo. Gently southward dipping strata of the ba-

saltic lower lapilli cone apron (LLCA) represent the flank of a large edifice, whereas radially dipping strata of the mugearitic to benmoreitic upper lapilli cone apron (ULCA) crudely define a smaller cone or apron.

Lower lapilli cone apron (LLCA, facies A)

Facies A-1

Facies A-1 is at least 200 m thick (Fig. 3). The base of the unit is not exposed. The massive to crudely bedded, shallow dipping (less than 20°) deposits of the LLCA are dominantly alkali basaltic to hawaiitic lapillistones containing abundant fragments of red algae. Juvenile clasts comprise formerly glassy now devitrified lapilli. Accidental clasts (<5 vol%) comprise lapilli and blocks of basalt, minor ankaramite, and rare amphibole-gabbro xenoliths. Isolated glassy crusted bombs and blocks with local impact sags are scattered throughout the deposit. Minor vitric ash and bomb horizons and lenses up to a few meters wide, that are rich in algal nodules, are intercalated. Overall, the succession is fines-poor. Thinly bedded to laminated deposits consisting of small sideromelane lapilli and ash make up <5 vol% of the LLCA. Juvenile clasts are blocky in shape and commonly bordered by curviplanar margins, though a few are slightly rounded and fluidally shaped. They are largely non- to moderately vesicular, with only rare highly vesicular pumice lapilli. Accretionary lapilli are up to 0.5 mm in diameter and include both concentrically layered and structureless types. They are found exclusively in fine-grained hyaloclastites. They are isolated or form clusters rather than beds. Oxidized scoria lapilli and ash occur exclusively in the uppermost section of the LLCA. The top of the basaltic LLCA is marked by a conglomerate horizon to be discussed later.

Interpretation. A submarine depositional site is suggested for the deposits of the LLCA because of:

1. the significant amount of admixed red algal debris, and
2. intercalated lenses of algal nodules (rhodoliths).

The lack of evidence for tractional processes indicates deposition in a sub-wavebase setting. This interpretation is not in conflict with the occurrence of algal nodules which generally need water movement to grow concentrically, because they can be frequently turned around by fishes (C. Betzler, personal communication). The rounding of some lapilli probably originated from abrasion within the conduit during eruption (Kano et al. 1996) rather than from shallow-water reworking, because rounded particles are very rare and scattered throughout the deposit rather than enriched in beds. Incipiently to moderately vesicular, blocky-shaped sideromelane lapilli and ash are typical products of explosive magma–water interaction, whereas highly vesicular sideromelane clasts reflect pyroclastic fragmentation (Fisher and Schmincke 1984; Houghton and Wilson 1989). It is highly probable that fragmentation occurred by a combination of exsolution of magmatic volatiles and hydroclastic processes which triggered additional disruption of vesiculated magma. The occurrence of accretionary lapilli indicates eruption plumes rich in condensed steam. The ash aggregates must have been sufficiently coherent to avoid disintegrating during water-settling and deposition in a marine environment. Moreover, impact sags are not restricted to subaerial deposits but were observed in submarine successions also (Cas et al. 1989; White 1996). The edifice might have breached the water surface during the late stage of the cone evolution, as indicated by the increasing amount of oxidized lapilli and rounded lapilli in beds near the top of the section.

Facies A-2

Monomict massive to crudely bedded intercalations within facies A-1 are up to a few tens of meters thick and up to ca. 100 m wide. They consist of hyaloclastite lapilli breccia that contains abundant irregularly-shaped bombs and lack matrix. Glassy blocky lapilli are incipiently to poorly vesicular. Scattered elongate bombs are up to 0.5 m long and account for ca. 10–20% of the breccia. The bombs are ragged in shape and their long axes are randomly oriented. They have non-vesicular, glassy rinds and commonly moderately vesicular (up to 40 vol%) interiors. The massive unwelded deposit is overlain by ca. 5 m thick, medium to thinly bedded ash-sized hyaloclastites. The hyaloclastites are locally slumped. Particles are blocky as well as fluidally shaped.

Interpretation. Facies A-2 is interpreted as a remnant of a small cone formed close to a vent in a shallow submarine setting. Volatile exsolution in the rising magma culminated in mild submarine lava fountaining to produce ragged water-chilled bombs and vesicular hyaloclastite breccia (Smith and Batiza 1989). Lava fountaining was probably not suppressed by the hydrostatic pressure in the shallow submarine setting (Staudigel and Schmincke 1984). Explosive magma–water interaction produced ash-sized blocky sideromelane shards while the formation of a steam plume probably facilitated the formation of fluidally shaped ash clasts. Such an eruption plume with inferred water-exclusion zones might also have contributed to the generation of ragged bombs resembling spatter fragments from subaerial lava fountains (Kokelaar 1986).

Upper lapilli cone apron (ULCA, facies B)

The upper lapilli cone is ca. 50–100 m thick and mugearitic to trachytic in composition as reflected in the pale color of relict glassy lapilli and low An-contents of plagioclase microphenocrysts (Schmidt 2000). The deposits are ash-poor, massive to poorly stratified, and consist of

juvenile glassy lapilli mixed with sparse country rock fragments, non-vesicular trachyte lapilli, and scattered glass-crusted bombs. The latter also occur in beds up to 3 m thick; matrix of glassy lapilli is minor. Juvenile glassy lapilli with 25–40 vol% of plagioclase microphenocrysts are non- to poorly vesicular, show trachytic texture, and have blocky shapes with curviplanar surfaces. Highly vesicular (up to 75 vol%) lapilli are restricted to the uppermost conglomeratic part of the succession. Lithic fragments make up <5 vol% of the deposits, but are enriched in some horizons. They consist dominantly of vesicular basaltic glassy lapilli derived from the LLCA. Lapilli and block-sized non-vesicular basalt and ankaramite fragments and fine-grained red algal fragments are minor. Non-volcanic rocks are restricted to:

1. a 6-m-wide and 2-m-thick patch reef deposit (site #1, Fig. 2) composed of rhodolith-coral-bivalve assemblages with abundant red algal laminite layers, and
2. 1–5-m-thick and up to 10-m-wide lenses of rhodolith-rich bioclastic sediments with scattered volcanic pebbles.

Interpretation

Blocky clast shapes of the glassy debris suggest phreatomagmatic explosions to have been the dominant fragmentation process (Fisher and Schmincke 1984). Beds enriched in lithic lapilli and blocks of directly underlying vesicular basaltic glassy lapilli (LLCA) suggest shallow-seated vent-widening explosive phreatomagmatic eruptions. The shallow submarine eruption and depositional environment is evidenced by the in situ patch reef and admixed red algal debris. The trachytic texture of plagioclase-rich glassy lapilli is evidence of a high degree of crystallization before fragmentation, possibly because of significant undercooling (rise of the liquidus temperature) in the underlying magma body as a result of degassing. We postulate explosive shattering and quench fragmentation of subaqueous extrusive domes to explain the coexistence of pumiceous lapilli, moderately vesiculated to pumiceous water-chilled bombs, and abundant highly crystallized lapilli. This interpretation remains speculative, however, because the source – a dome of intermediate composition – is not exposed. A 5-m-wide columnar body, circular in plan view, of benmoreitic composition penetrating the clastic rocks of the ULCA is thought to represent a feeder conduit. In summary, the radially dipping strata of the evolved ULCA define a single cone/apron which probably originated from combined phreatomagmatic eruptions and shattering of submarine extrusive domes.

Deposits of a shattered submarine trachytic dome (facies B)

A spectacular channel-confined trachytic volcaniclastic succession (site #2, Fig. 2) comprises:

1. coarse-grained breccia of non-vesicular glassy and crystalline trachyte (facies B-1);
2. pumice-rich breccia (facies B-2); and
3. crystal-rich volcaniclastic sandstone (facies B-3).

This facies association is up to 50–60 m thick and exposed for ca. 350 m in the north-south direction in close proximity to two trachytic domes to the north and east, respectively.

The massive *coarse-grained breccia* (facies B-1) is clast-supported; juvenile clasts are either glassy or crystalline and range from approximately 1 cm up to 1 m in size. Tube pumice clasts seem to be rare but their abundance might be underestimated because many clasts are altered to a whitish chalky rock with obscured primary textures. Minor sandy matrix is composed of similar clasts mixed with broken crystals and fossil debris (e.g. *Amphistegina* sp., coralline red algae). Many larger clasts show tiny normal joints along the outer margins, whereas the interior is usually polyhedrally jointed (Fig. 4a).

The *pumice-rich breccia* (facies B-2) shows gradational contacts to the coarse-grained breccia described above. It is clast-supported and contains abundant pumice lapilli and blocks mixed with non-vesicular glassy and minor crystalline clasts. The pumice fragments are up to 0.5 m in length and are either equant, elongate, or ragged in shape. Finer-grained beds of well-preserved small lapilli contain up to 70–80 vol% of tube pumice clasts. Matrix of fine ash is rare (Fig. 4d). Vesicularity of the pumice lapilli is estimated to be up to 70 vol%, with minor non- to poorly vesiculated clasts (Fig. 4b, c). Sigmoidal outsized clasts up to 15 cm long occur in some horizons (Fig. 4e), with their long axes lying parallel to stratification. Particle terminations are both ragged and smooth where strongly compacted. Some clasts have quenched margins and relict tube-pumice textures (Fig. 4e).

The *crystal-rich volcaniclastic sandstone* (facies B-3) forms thin- to medium bedded, well-sorted deposits composed of broken crystals of plagioclase, amphibole, rare phlogopite, and very rare, strongly resorbed, clinopyroxene. The crystals are mixed with glassy and crystallized ash- to fine lapilli-sized trachyte and minor fragments of coralline red algae. Glassy, crystalline, and pumiceous trachytic lapilli are intercalated with the crystal-rich sandstone.

Interpretation

The coarse breccia facies is interpreted as representing the proximal deposit of a collapsed and/or explosively shattered outer margin of a steep-sided submarine trachytic dome which had breached the sediment surface. Variably vesicular clasts of the coarse breccia indicate substantial degassing before emergence. Avalanching of debris from the solidified non-vesicular glassy and pumiceous margin of the dome was most likely triggered by

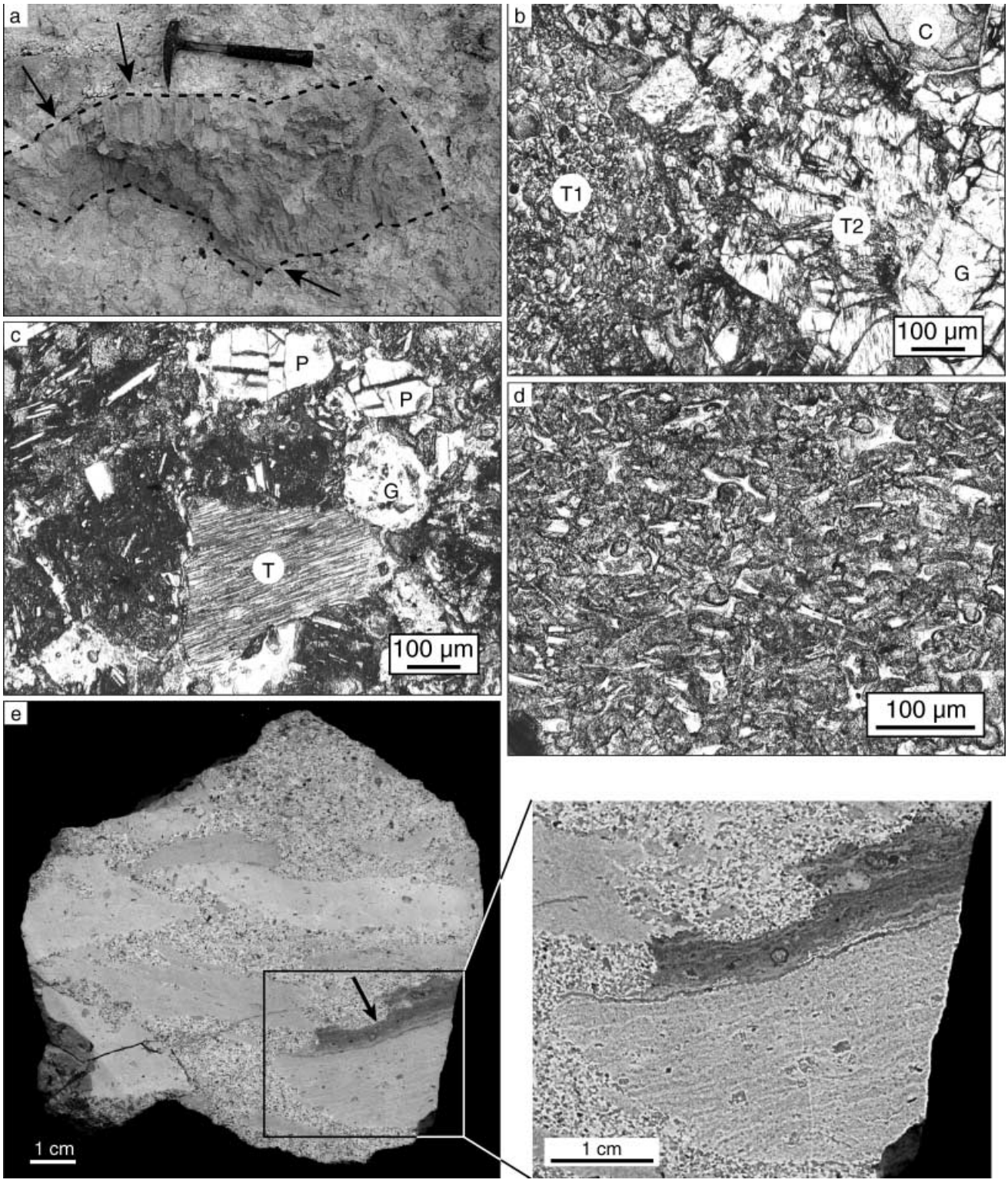

Fig. 4a–e Channel deposit (facies B, site #2, Fig. 2). **a** Trachytic block with fracture-controlled surfaces and tiny normal joints along the margins (*arrows*) set in a coarse-grained hydroclastic breccia composed of non-vesicular glassy and crystallized and pumiceous trachyte (facies B-1). Hammer for scale. **b–d** Photomicrographs of fine-grained pumice-rich trachyte breccia (facies B-2). Plane polarized light. **b** Juvenile clasts of variable vesicularities including highly vesicular pumice lapilli (*T1*), tube pumice clasts (*T2*), and non-vesicular glassy lapilli (*G*). Note fine vesicles of *T2* compared with *T1*. *Upper right corner* micritic carbonate clast (*C*). **c** Broken plagioclase crystals (*P*), non-vesicular glass lapilli (*G*), and highly vesicular tube pumice lapilli (*T*) set in an altered hydroclastic matrix. **d** Bubble wall- and bubble junction shards. **e** Sawn and polished specimen of pumice-rich breccia (facies B-2). Sigmoidal trachytic pumice clasts set in a matrix of ash to fine lapilli. Large clasts have ragged or wispy terminations and may show relict glassy crusts (*arrow*). Close-up shows relict tube pumice texture indicated by the foliation parallel to the long axis of the clast

oversteepening of the dome. Unroofing of the dome led to a sudden decrease in pressure in its interior giving rise to sudden exsolution of volatiles resulting in pyroclastic fragmentation. Deposits inferred to have originated during pyroclastic explosions are the pumice-rich breccia and the crystal-rich sandstone (cf. Cas et al. 1990). Explosions must have been very vigorous as indicated by abundant broken crystals and fine-grained bubble-wall shards. Sigmoidal clasts (Fig. 4e) are interpreted as having formed during explosive rupturing of pumiceous, still ductile parts beneath the cooled carapace of the dome. The first-order driving mechanism for the explosion was probably exsolution of volatiles but further fragmentation by magma–water interaction and/or quench fragmentation cannot be ruled out, although the chilled margins of pumice clasts might have been formed solely by chilling.

The volcaniclastic deposits resemble those described by Cas et al. (1990) and Scutter et al. (1998) in many aspects, both successions likely to be associated with the submarine emplacement of felsic lava flows and domes.

Deposits of the littoral setting

Non- to incipiently vesiculated fluidally shaped bombs (spatter) and coarse to medium-sized lapilli mixed with crystalline lithics of similar grain size form massive to very crudely bedded deposits at the eastern coast of Porto Santo (site #3). The deposits are up to 2 m thick and a few meters wide, and occur in isolated outcrops on the beach or interbedded with pillow-hyaloclastite breccia of the lava delta (described below). Ash-sized tachylite and sideromelane fragments and scattered broken crystals and microcrystalline basalt clasts are mixed with the pillow-hyaloclastite breccia or form local very thin-bedded to laminated intercalations. Beds or lenses are up to 20 cm thick and laterally traceable up to a few meters. Both, sideromelane and tachylite ash grains are non- to poorly vesicular and fluidally shaped, although many are broken. Some resemble droplets, others are amoeboidal. The fluidally shaped clasts contrast strongly with blocky-shaped particles of the pillow-hyaloclastite breccia.

Interpretation

This facies association is interpreted as representing ejecta of littoral cones that were formed by steam explosions in a littoral environment when high-energy surf drove water into ruptured active lava tubes (Fisher 1968; Mattox and Mangan 1997). The spatter is interpreted as having formed as a result of bubble-burst activity triggered by abrupt fracturing of active lava tubes, whereas glassy lithic debris forms when incandescent lava tubes fracture and come into contact with the surf (Mattox and Mangan 1997). The fluidally shaped ash clasts might have originated from tephra jets caused by small explosions formed when the consolidated skin of littoral lava tubes sloughed off and fluidal lava within was exposed to the surf. The ejecta might have formed during localized steam explosions rather than large-scale tephra jets produced by bench collapses (Mattox and Mangan 1997), because the deposit is very restricted laterally. The fluidal clast shapes are because of the surface tension of low-viscosity lava during flight through the air. Equant blocky clasts can form by break-up of originally fluidally shaped clasts during flight or when impacting the ground (Fisher 1968; Fisher and Schmincke 1984).

The deposits formed at the shoreline but must have been emplaced below sea level, because they are intercalated with subaqueously emplaced pillow-hyaloclastite breccia. They are interpreted as the submarine counterpart of subaerially emplaced littoral half-cones at the leading edge of active lava deltas at the shoreline.

Subaerial deposits

Scoria cones (facies C)

Eroded remnants of at least nine basaltic cones up to ca. 300 m in diameter are composed of intercalated lava flows and related scoriaceous breccia, bomb-, block-, lapilli-, and ash deposits. The central red parts of the cones are thermally oxidized. Oxidized spindle-shaped and bread-crusted bombs and agglutinated spatter are rare. Monomict basaltic scoriaceous lapilli, ash and minor bomb deposits are relatively well-sorted and poorly stratified. Some beds are enriched in blocky sideromelane clasts. The deposits form laterally continuous, horizontal to gently dipping beds up to 2 m thick sandwiched between lava flows. Top contacts are commonly baked by overlying lava flows.

Interpretation The scoria deposits are interpreted as having been formed by pyroclastic fragmentation of basaltic magma, as a result of mildly explosive Hawaiian and/or Strombolian eruptions in a subaerial setting. Red spindle- and bread-crust bombs and slightly agglutinated spatter indicate thermal oxidation and welding proximal to active vents. The shape (e.g. spindle bombs) and surface features (bread crust) of the fragments indicate transport through air before deposition. Lapilli and coarse ash beds characterized by relatively good sorting and mantle-bedding are indicative of medial to distal airfall deposits. The few beds enriched in blocky sideromelane clasts with variable vesicularities reflects significant impact of external water as the mechanism driving fragmentation. Thus, explosions might have been partly phreatomagmatic.

Tuff cones

Subaerial tuff cones or tuff rings originating from phreatomagmatic explosive activity are abundant along the coasts of volcanic islands (Vespermann and

Schmincke 2000). An erosional remnant of a tuff cone or tuff ring with an estimated preserved thickness of 40–50 m occurs in an inaccessible vertical cliff section at the eastern coast of Porto Santo (site #4, Fig. 2). The deposits are yellowish, fine-grained, thinly bedded, and underlie scoria cone deposits. Observations were made by means of binoculars.

Armored lapilli occur in a single, strongly weathered horizon just beneath the base of a subaerial lava flow in southeastern Porto Santo (site #5, Fig. 2). Cores of the armored lapilli are composed almost exclusively of variably vesiculated tachylite. Ash rims are commonly structureless. These deposits are interpreted as having originated from wet surges.

Deposits resulting from effusive processes

Submarine trachytic effusive activity (facies D)

Trachytic submarine effusive activity is represented by a massive bed ca. 10 m thick composed of non-vesicular pillow lobes of trachyte (facies D-1) located in northeastern Porto Santo (site #6, Fig. 2). Some pillow lobes have penetrated into the underlying basaltic hyaloclastites. The pillow tubes are up to 1.5 m in diameter but are more extensive in longitudinal section. The pillows, which are light grayish to pale pink with white margins, some with tiny normal joints along the margins, are set in a clast-supported coarse-grained whitish lapilli breccia of similar composition. The massive pillow horizon grades downslope into a pillow fragment breccia.

A second trachytic lava flow (facies D-2) in southeastern Porto Santo (site #7, Fig. 2) covers an area of ca. 250×500 m with an exposed thickness of at least 5 m. The massive coherent flow might be more extensive and thicker, because its base and top are poorly exposed. Poorly exposed margins of the lava flow are marked by:

1. massive monomict trachytic breccia at least ca. 5 m thick composed of coarse lapilli-sized crystallized, glassy, and pumiceous angular clasts exhibiting jigsaw- to clast-rotated texture (facies D-2a), and
2. pillow-shaped protrusions with tiny normal joints.

Lava flow and massive pumice-lithic breccia are mantled by a dominantly lenticular, commonly inversely graded, pumice-lithic breccia (facies D-2b) composed of lapilli-sized angular to subrounded clasts of crystallized trachyte, slightly vesicular flow-banded obsidian, and pumice. Beach pebbles, lapilli of the ULCA, and fragments of coralline algae are rare. Fragments of laminated well-sorted crystal-rich volcaniclastic sandstone are scattered throughout the breccia. The sandstone consists of blocky glassy clasts intermixed with abundant plagioclase fragments. The bedded breccia is closely associated with up to 15×5 m wide rhodolith reefs and detrital rhodolith- and coral-bearing limestone.

Interpretation

The pillow succession from site #6 (facies D-1) is interpreted as a submarine trachytic lava flow probably fed by the fluid interior of the extrusive trachytic dome described above (Fink and Anderson 2000). The lapilli breccia and the pillow fragment breccia originated from quench fragmentation, as a result of thermal shock of lava in contact with seawater. The trachyte magma is thought to have been anomalously hot to generate a pillowed flow and to explain the small dimensions of the pillow lobes (Furnes et al. 1985; Yamagishi and Dimroth 1985; Walker 1992).

The lava flow from site #7 (facies D-2) and associated breccia facies are also interpreted to have been emplaced under water. Despite the limited areal extent, the succession is very similar to the voluminous submarine rhyolite lava flow of Ponza Island (Italy) (Scutter et al. 1998). Similarly high eruption temperatures, with resulting low viscosity, can be inferred, because marginal pillows only reach up to 1 m in diameter. A low viscosity is also suggested by the lack of trachytic texture or microshear zones typical of laminar flow of viscous material (Smith et al. 1993). The marginal massive breccia (facies D-2a) was produced by quench fragmentation of the outermost crust of the lava flow. Jigsaw texture is restricted to narrow zones along the contact between lava flow and breccia, indicative of in situ fragmentation. The mantling massive glassy clast breccia is interpreted as having been produced by quench fragmentation and autobrecciation of the advancing layered lava flow, which was composed of a crystallized interior, an obsidian layer, and a variably vesiculated margin. The lenticular, finer-grained breccia (facies D-2b) originated from reworking and subsequent redeposition by fragments of the mantling glassy breccia. Abundant broken crystals in the volcaniclastic sandstone indicate explosive activity within the advancing lava flow (Fink and Manley 1989).

Submarine basaltic effusive activity

The base of a ca. 15-m-high coastal cliff at the southwestern tip of Porto Santo consists of massive, irregularly to columnar jointed protrusions of almost vertically orientated to slightly inclined layers of basalt set in a hyaloclastite breccia (Fig. 5). Many dike (?) terminations are pillow-shaped. The protrusions fan out to produce numerous thin and imbricated slabs with single sheets of a few meters in lateral extent but no more than 30 cm thick. Slabs are dissected by tiny normal joints and form convex-upward curves. The slabs are associated with a monomict, massive, coarse-grained, clast-supported breccia composed of angular lapilli of similar basalt. The fragments locally show jigsaw texture. Pillow-shaped bodies are scattered throughout the breccia, with some attached to the slabs. Carbonate-cemented volcaniclastic sandstone, which locally grades into fossiliferous sandstone, is locally intermixed with the breccia.

Interpretation

The facies association and the inclination of the slabs and closely packed pillows define the flank of a compound submarine pillow-sheet flow-breccia cone, inferred to have been emplaced during submarine effusive activity. Imbrication of the slabs and pillows attached to the slabs indicate simultaneous vertical and lateral accretion. Jigsaw texture observed in the monomict breccia is indicative of in-situ quench fragmentation.

Subaerial effusive activity

Columnar-jointed basaltic lava flows (facies C) occur in western and eastern Porto Santo high in the stratigraphic section (Fig. 3). They form ca. 1–5 m thick and laterally continuous sheets which are horizontal or dip gently seaward. The basalt flows are incipiently to moderately vesiculated. The flows are separated by red oxidized scoriaceous lapilli breccia in matrix-poor layers up to ca. 1 m thick. The breccia between the lava flows is interpreted as autobrecciated flow tops and flow bases formed in a subaerial environment.

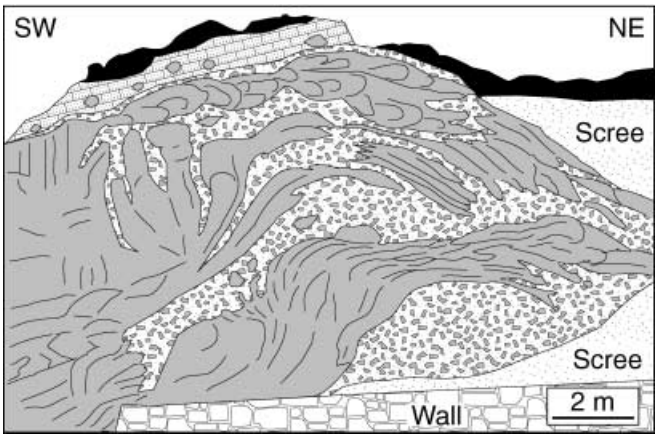

Fig. 5 Basaltic feeder dike connected to a small submarine compound pillow-sheet flow-breccia cone overlain by a white, fossiliferous sandstone (*white*) with scattered basalt pebbles, cobbles, and boulders (*gray*). Top of cliff made of columnar jointed basaltic lava flow (*black*) (southwestern tip of Porto Santo)

Lava flows that entered the sea (facies E)

The eroded remnants of the submarine lapilli cone aprons (LLCA, ULCA) are overlain by an up to 200-m-thick basaltic succession composed of glassy fragmental rocks and associated coherent pillow lava and sheet flow lava. The boundary between the lapilli cone succession and the basaltic lava delta is exposed along the eastern coast of Porto Santo.

West-coast of Porto Santo

Massive gently seaward-dipping lava flows and closely packed pillow lava dominate the lower part of the cliffs along the southwestern coast of Porto Santo. This facies has a maximum thickness of 50 m. Single tabular lava flows are up to 15 m thick, whereas pillow units reach up to 20 m in thickness. The succession is associated with hyaloclastite breccia, beach boulder horizons, and fossiliferous sandstones (Fig. 6). The lava flows lack scoriaceous top and basal breccia and commonly show columnar jointing, with entablature jointing restricted to thin lava flows and to marginal domains of thick lava flows. The surfaces of lava flows are smooth to highly irregular, and some are coated by deposits of algal mats up to 1 cm thick. Pockets of carbonate-cemented glassy lapilli

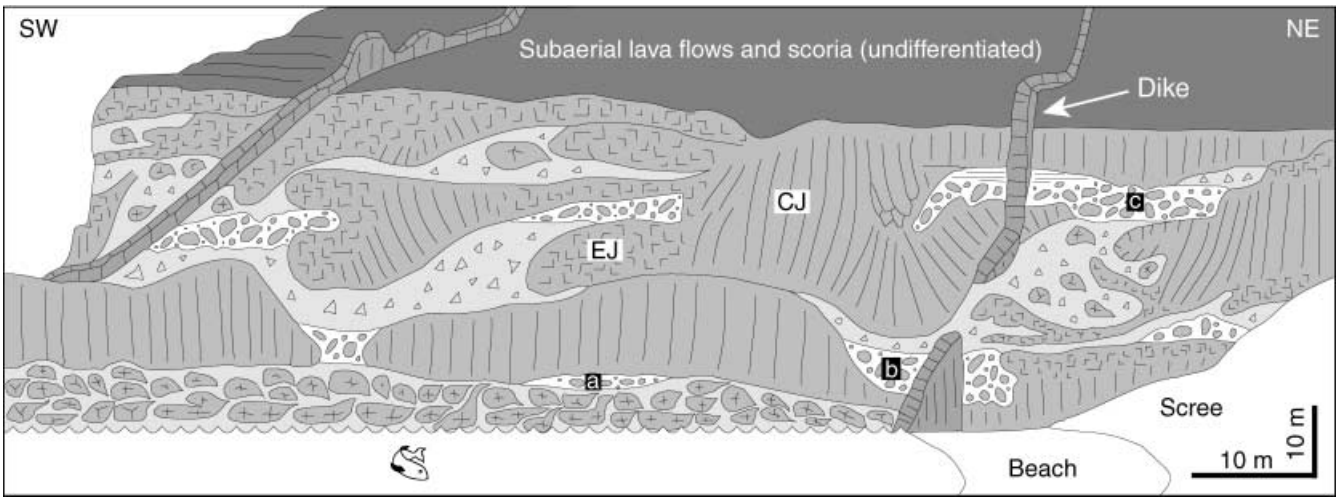

Fig. 6 Basaltic lava delta (facies E) along the southwestern coast of Porto Santo. The succession is composed of pillow lava (base) and thick tabular lava flows with associated hyaloclastite breccia (*triangles*), intercalated with three boulder horizons (*a*, *b*, *c*). Note entablature jointing (*EJ*) and columnar jointing (*CJ*) of lava flows. Only the submarine part is illustrated

locally infill irregularly shaped cavities on top of jagged lava flow surfaces. The deposits are locally thinly bedded, but more commonly they are massive. The clasts are composed of non- to poorly vesiculated lapilli of palagonite, sideromelane lapilli being rare. Lapilli commonly show smooth, fluidal surfaces, some bordered by broken vesicle walls, although blocky clasts are present in subordinate proportions. Pillow lavas define an irregular framework of interconnected lava tubes. Intersticies of pillow tubes are filled with fine-grained hyaloclastite and/or fossiliferous sandstone or mudstone.

Interpretation. The facies association comprising tabular lava flows, pillow lava associated with genetically related hydroclastic breccia, and beach boulder conglomerates indicates submarine emplacement of the lavas in a shallow nearshore environment, which extends from the low tide level out to the depth of fair weather wavebase. Minor fragmentation of thick subhorizontal lava flows is strong evidence of prolonged effusions and emplacement of the flows on gentle offshore slopes limiting the formation of pillow lava and fragmentation into hyaloclastite breccia. The latter is supposed to form where seafloor topography locally steepened (Schmincke et al. 1997). The resulting lava delta consists of a single massive structural unit dominated by coherent lava facies. The subaerial eruption of thick lava flows was accompanied by lava fountaining. So erupted sideromelane lapilli were subaqueously emplaced and subsequently redeposited within wave base filling up irregular depressions on top of the flows.

East-coast of Porto Santo

A foreset-bedded wedge of glassy fragmental basaltic rocks dominates the eastern coast, and extends about 2 km inland (Fig. 2). It thickens coastward to the east while pinching out against the erosional remnant of the tephra cones (LLCA, ULCA) to the west (Figs. 7 and 8a). The wedge can be subdivided into several basaltic units, which are separated by layers comprising erosional debris of the LLCA and the ULCA, fossiliferous calcarenites and biomicrites, and debris flow deposits of epiclastic sand, gravel, and boulders.

Each basaltic unit consists of pillow-hyaloclastite breccia (A) and pillow fragment breccia (B) with minor intercalated lava flows (C). Fragmental rocks, dominated by pillow-hyaloclastite breccia, are estimated to make up 70–80 vol% of the entire wedge. Boundaries between lava flows and clastic rocks are gradational.

Each lava/breccia unit is characterized by foreset beds which generally dip coastward, although the dip direction can be very irregular on a small scale. Inclination of foreset beds ranges from 5–40°, averaging 15–30°. Small-scale listric faults with displacement up to 2 m are rare. The foreset-bedded lava/breccia units are overlain by subhorizontal lava flows with their lower surfaces merging with lava tubes that descend the foresets

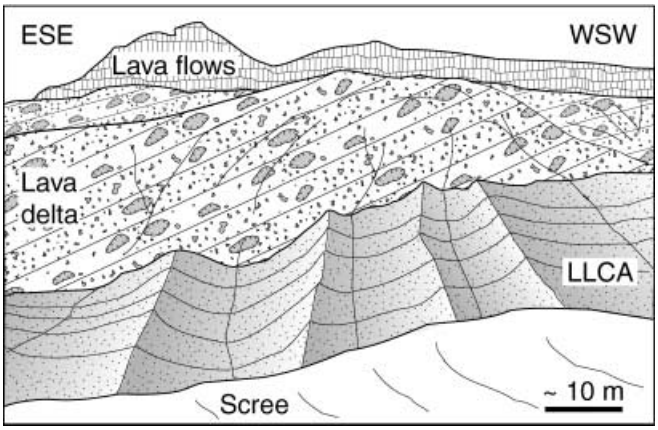

Fig. 7 Wedge-shaped basaltic lava delta succession pinching out against the erosional remnant of the LLCA. Background: subaerial lava flows, foreground: scree. East Porto Santo (site #9, Fig. 2)

(Fig. 9). Basaltic lava/breccia units comprise the following facies:

1. Pillow-hyaloclastite breccia is composed of:
   a) angular glassy lapilli, both sideromelane and tachylite,
   b) intact or broken pillow-shaped bodies, and
   c) crystalline basalt lapilli.

   Finer-grained hyaloclastite matrix is subordinate. The breccia is moderately sorted, clast-supported, and massive to poorly stratified, with gradational contacts to pillow fragment breccia and various types of lava flow (Fig. 1c). Juvenile particles are non-vesicular (0–5 vol%) glassy basalt, and are characterized by abundant plagioclase quench microphenocrysts (20–40 vol%) as indicated by swallow-tail terminations. Small glassy lapilli are generally blocky in shape with curviplanar surfaces. Isolated pillow-shaped bodies are a few centimeters up to ca. 0.5 m in diameter, entirely to partly surrounded by glassy crust, and tubular-, sack-like-, or fluidal in shape (Fig. 1b, c). Most pillows are non-vesicular, but cores of some small pillows are variably vesicular and have central cavities. Incipiently vesicular crystalline basaltic lapilli are scattered throughout the pillow-hyaloclastite breccia and may form up to ca. 10–20 vol% of poorly defined beds. The clasts are subangular to rounded, with vesicles filled by carbonate.
2. Pillow fragment breccias consist of deposits of relatively close-packed pillow fragments that grade into isolated broken pillow fragments and hyaloclastite breccia showing jigsaw- to clast-rotated textures (Fog. 1d). The pillow fragment breccia is set in a matrix of hyaloclastite breccia. Beds comprise clast-supported poorly sorted deposits with gradational contacts to foreset-bedded hyaloclastite breccia and sheet flows. Broken and intact pillows intermixed with angular glassy lapilli and blocks locally form massive coarse-grained, laterally discontinuous, wedge-shaped bodies.

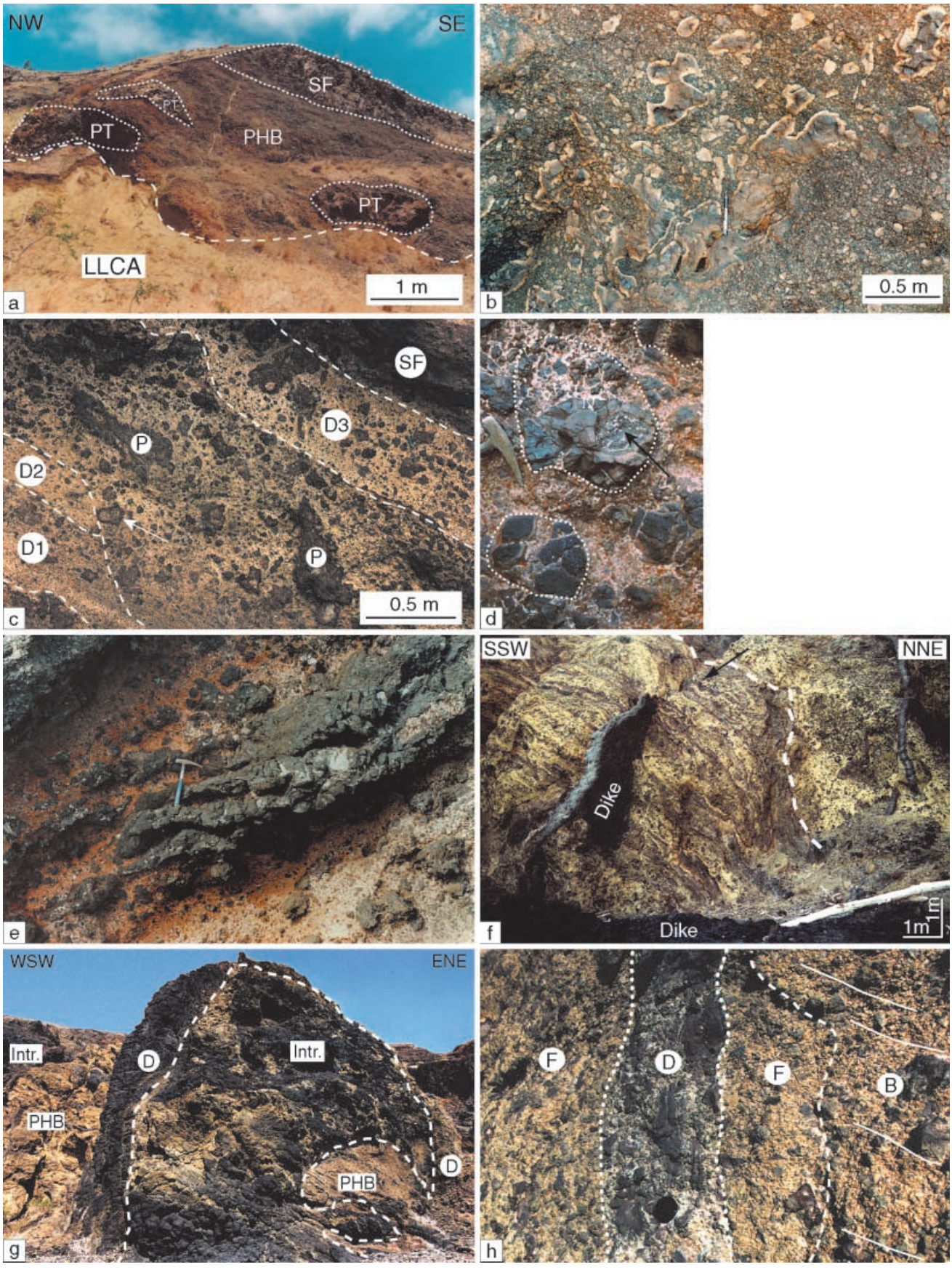
NW
SE
SF
PT
PT
PHB
PT
LLCA
1 m
a
0.5 m
b
SF
D3
P
D2
D1
P
0.5 m
c
d
e
SSW
NNE
Dike
Dike
1m
f
WSW
ENE
Intr.
D
Intr.
PHB
D
PHB
g
F
D
F
B
h

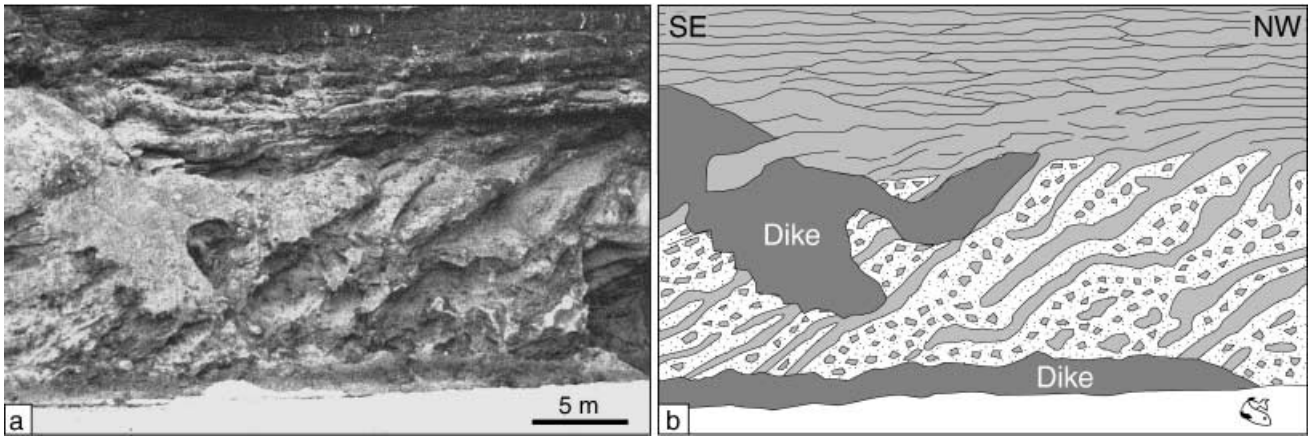

Fig. 9 **a** Structural relationship between foreset-bedded, steeply dipping pillow-hyaloclastite breccia overlain by subhorizontal lava flows. Note that lava tubes of the foreset-bedded unit are attached to the flat-lying lava flows. **b** Sketch of a. Cliff section of the central northern coast of Ilhéu de Cima located ca. 0.5 km southeast of Porto Santo. View to the south. Lower 20 m of the section are shown (site #10, Fig. 2)

3. Sheet flows (0.1–1 m thick), massive tabular lava flows (<5 m thick), and *lava tubes* are intercalated with the fragmental deposits. The sheet flows show pinch-and-swell structures, are laterally discontinuous, and locally grade into hyaloclastite breccia. Tabular lava flows are traceable up to 40–50 m. Finger-like injections into the underlying pillow-hyaloclastite breccia are common. Many lava tubes have irregular margins with trap door- and toothpaste-pillows on top of the flows and injections from the bottom of the flow into the underlying breccia (Fig. 1e). Closely packed pillow lava composed of elongate, slightly inclined pillow tubes is rare in this area.

◀ **Fig. 8a–h** Lava delta succession of eastern Porto Santo (site # refer to Fig. 2). **a** Erosional unconformity (*dashed line*) between reworked LLCA (base) and basaltic lava delta sequence. PHB (clastic facies): pillow-hyaloclastite breccia; *PT* pillow tube, *SF* sheet flow (coherent facies) (site #11). **b** Non-vesicular amoeboid pillows set in foreset-bedded hyaloclastite breccia. The irregular shape of the pillows indicates drainage of extraordinarily hot and fluid lava from tubes on steep slopes. Pale yellow margins are weathered, formerly glassy crusts (site #3). **c** Pillow-hyaloclastite breccia with scattered, irregularly shaped pillows (*P*) intermixed with glassy lapilli. Yellow "matrix" is clay resulting from alteration of glassy lapilli. Note small globular pillow (*white arrow*) entirely surrounded by a glassy margin. *D1*, *D2*, and *D3* are reversely graded monomict debris flow deposits. *Upper right corner* is a sheet flow (*SF*) (site #3). **d** Pillow fragment breccia (site #3). Three pillow fragments are outlined. Note vesicular core (*arrow*) and jigsaw-fit breccia of pillow in the center. Glass crust is well preserved at pillow in the lower right. Hammer for scale. **e** Lava tongue with frayed edges and margins set in a monomict carbonate-cemented hyaloclastite breccia (site #3). **f–h** Syn-volcanic intrusions within basaltic lava delta (site #3). **f** Peperitic intrusive complex of fragmented dikes and sills. The *dashed line* approximately marks the boundary between intrusives (*lower left*) and foreset-bedded pillow-hyaloclastite breccia (*upper right*). Note bending of sill (*arrowed*). **g** Irregularly shaped composite syn-volcanic basaltic intrusion (*dotted line*) penetrating pillow-hyaloclastite breccia (*PHB*). Note a second intrusion (*Intr.*) in *upper left corner*. Later dikes (*D*) border the syn-volcanic intrusion. Width of photograph is ca. 30 m. **h** Peperitic dike within pillow-hyaloclastite breccia. Completely fragmented dike (*D*), outlined by *dotted line*, composed of glassy clasts; large fragments show multiple quench crusts. Fluidized host rock (*F*) which lacks bedding admixed with dike clasts. Unaffected pillow-hyaloclastite breccia (*B*) shows crude bedding accentuated by white lines. Lens cap is 5 cm in diameter

Interpretation. Foreset-bedded pillow-hyaloclastite breccia overlain by subhorizontal lava flows originated from subaerially erupted low-viscosity basaltic lava flows that entered the sea to form a structurally bipartite lava delta (Moore et al. 1973; Schmincke et al. 1997). Several lines of evidence argue for subaerial eruption and submarine deposition of the lava flows. Firstly, abundant plagioclase microlites in the glassy crust demonstrate that lava flows had thoroughly degassed and partially crystallized during subaerial flow before quenching on contact with seawater (Moore 1970, 1975). Significant degassing is further supported by non-vesicular juvenile particles and pillows. In contrast, shallow submarine eruptions commonly produce clasts of variable vesicularities (Fisher and Schmincke 1984) and vesicular pillows (Jones 1969; Moore 1970). Secondly, red scoria lapilli are indicative of thermal oxidation and autobrecciation during subaerial flow. Minor globular pillows that have a vesicular core indicate quenching before peak vesiculation and thus could have originated from shallow submarine eruptions (Jones 1969), probably fed from small vents rooted in the lava delta.

Submarine slopes must have been:

1. highly irregular, supported by variable dip directions, and
2. steep, as indicated by, e.g., the high degree of fragmental glassy debris, steeply inclined foreset beds, and isolated pillow sacks.

The deposits probably originated from a combination of fragmentation mechanisms including the following three end members (Batiza and White 2000):

1. thermal-shock granulation (quench fragmentation) operating during contact of lava with seawater to produce glassy breccia;

2. spall fragmentation results in hyaloclastites because of disruption of the solidified glassy crust as the interior of the flow advances; and
3. impact shattering (mechanical fragmentation) of detached pillow sacks during downslope avalanching which produces pillow-fragment breccia, glassy breccia, and, if transported farther, crystallized fragments representing holocrystalline interiors of pillows.

Explosive fragmentation might also have occurred (cf. deposits of the littoral setting).

Assuming submarine slopes of constant steepness, variable facies such as glassy breccia, pillow fragment breccia, pillow lava (lava tubes), and sheet- and tabular lava flows are interpreted as reflecting increasing lava supply (mass eruption) rates.

Lava deltas contain two main structural units (e.g. Moore et al. 1973). The lower steeply inclined foreset-bedded unit (Fig. 1c) represents a hyaloclastite breccia prism, and is capped by subhorizontal lava flows (topset beds) representing the upper structural unit (Fig. 9). The lower flows are inferred to have been subaqueously formed, whereas the upper ones were emplaced subaerially. The boundary between foreset-bedded units and topset beds is gradational because horizontal lava tubes can bend downwards at the seaward end of the hydroclastic prism to extend down the submarine slope (Fig. 9). This "passage zone" is generally interpreted as representing the sea level at the time of its formation (Jones and Nelson 1970; Schmincke et al. 1997). Rarely preserved accumulations of coarse-grained glassy debris originated from avalanching down the steep slopes, with deposition where the slope gradient decreased, and can be interpreted as talus deposits or coarse bottom sets (Porebski and Gradzinski 1990).

Intrusive processes

Intrusions were emplaced throughout volcanic activity and are subdivided into:

1. syn-volcanic intrusions within the lapilli cone aprons,
2. syn-volcanic intrusions within the lava delta succession, and
3. later intrusions.

Syn-volcanic intrusions within the lapilli cone aprons (facies F)

The LLCA and ULCA in northeastern Porto Santo are penetrated by four dome-shaped columnar-jointed trachytic to rhyolitic intrusions 200–500 m in diameter (Fig. 2). At the northeastern tip of Porto Santo, coastal cliffs expose vertical sections through two trachytic intrusions each ca. 250 m thick. Original dimensions must have been much larger, because all domes are deeply eroded and basal contacts are not exposed.

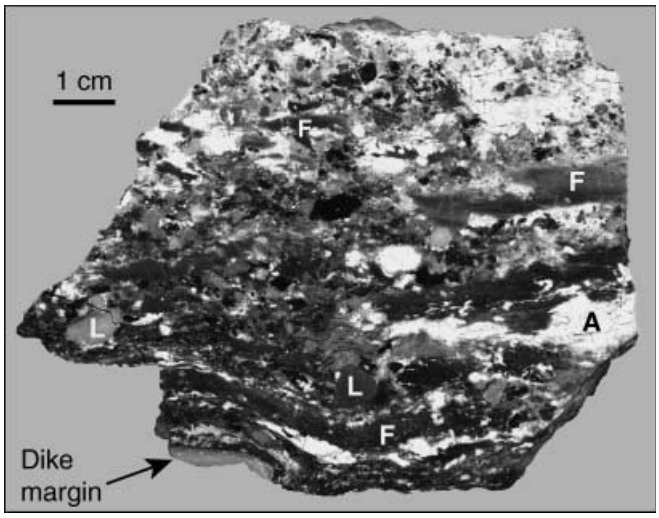

Fig. 10 Polished hand specimen of pumice-lithic trachyte breccia (facies D-2b) showing well-developed eutaxitic texture in close contact with adjacent dike (*arrow*). Foliation caused by secondary welding is dike-parallel and dies away from the dike. Note wrapping of trachytic glass bands (*F*) around lithics (*L*). Alteration of glass produced white-colored clay (*A*). South Porto Santo (site #8, Fig. 2)

Margins of the trachytic to rhyolitic domes are marked by glassy breccia with jigsaw- to clast-rotated texture and/or pillows indicating intrusion into unconsolidated water-saturated host rock. Thus, emplacement of the intrusions must have been essentially coeval with deposition of the host sequence.

Features of a single dike (site #8, Fig. 2) that penetrates the pumice-lithic breccia further supports syn-volcanic intrusive activity. Primary bedding of the pumice-lithic breccia described above (facies D-2b) is destroyed adjacent to the dike and replaced by a well-developed eutaxitic texture (Fig. 10) which parallels the dike and extends as far as 10–15 cm from the contact with the dike. There is a gradual transition from unaffected finely vesicular tube pumice clasts to strongly flattened and elongate relict pumice clasts towards the dike contact. Aligned relict pumice clasts coalesce close to the dike contact to produce dark undulating plastically deformed bands up to 1 cm thick which wrap around rigid particles (lithic clasts, non-vesicular glassy clasts, crystals) (Fig. 10). In thin section, macroscopically dark bands, and single sigmoidal clasts, are composed of pale brown glass with plagioclase microlites (Fig. 11a). Formerly tubular vesicles are compacted, and locally produce a flow-banded texture parallel to the dike. Clay-filled round to ovoid amygdules up to 1 mm in diameter occur locally (Fig. 11b), and represent vesicles generated by secondary vesiculation during reheating of the host rock by the dike (Schmincke 1967; McPhie and Hunns 1995). Abundant plagioclase phenocrysts are either euhedral or, more commonly, fractured to a jigsaw-fit puzzle indicating that they were broken in-situ (Fig. 11b). The margin of the glass bands and flattened clasts is often flow-

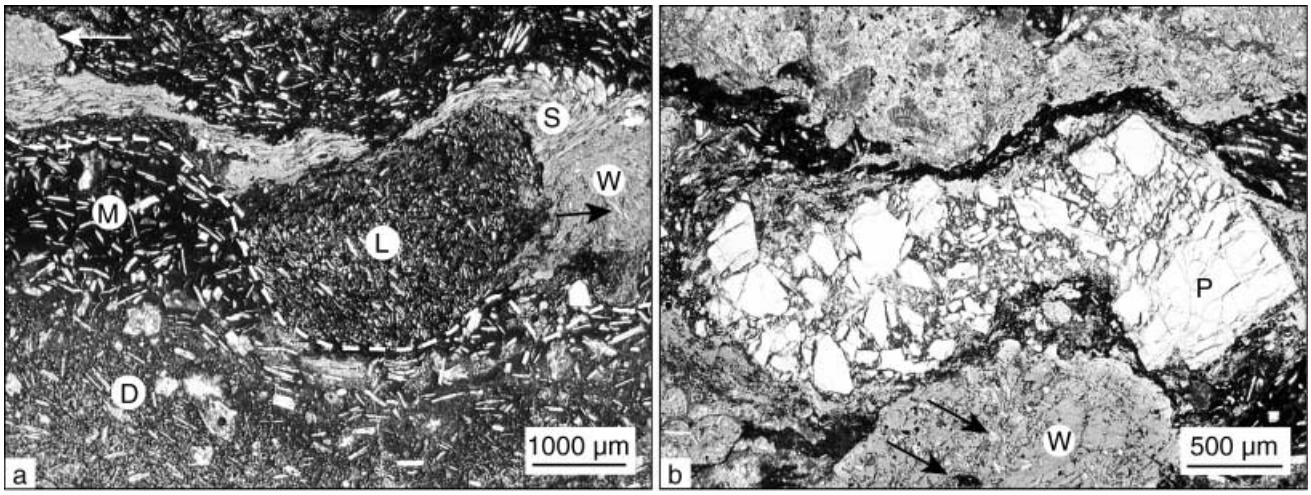

Fig. 11a,b Photomicrographs of pumice-lithic breccia close to the contact to adjacent dike. Plane polarized light. South-Porto Santo (site #8, Fig. 2). **a** Contact dike/pumice-lithic breccia showing sheared/lensoid (*S*) and massive (*W*) zones of secondary welded pumice wrapped around lithic clast (*L*). The glass contains abundant plagioclase microlites (*arrowed*). *Dashed line* marks the boundary between secondary welded breccia (*above*) and dike (*below*). Note chilled margin (*M*) of finely vesiculated plagioclase-phyric dike (*D*). **b** In situ brittle deformation of plagioclase phenocryst (*P*) showing jigsaw-fit texture. Deformation was caused by directed shear stress during injection of the dike. Note clay-filled vesicles (*arrowed*) in secondary welded glass (*W*). Black schlieren are thermally baked matrix and lithic clasts

banded parallel to the dike and/or characterized by a jigsaw-fit puzzle of lensoid glassy fragments (Fig. 11a). Plastically deformed elongate pumice fragments and brittle deformation of plagioclase phenocrysts indicate significant heat transfer into the sediment adjacent to the dike and strong shear stress during its emplacement. The textures described above exactly match those described by McPhie and Hunns (1995) from Mount Chalmers, Queensland (Australia) and are similarly interpreted as having formed by secondary welding of unconsolidated water-saturated pumice-lithic breccia close to the contact with the dike.

Syn-volcanic intrusions within the lava delta succession (East Porto Santo)

The basaltic lava delta succession is intruded by at least two generations of dikes/sills and one dome-shaped intrusion, which are well exposed in cliffs along the eastern coast of Porto Santo (site #3, Fig. 2). Intrusions account for approximately 10–15 vol% of the lava delta sequence.

The *first generation* intrusions comprise subvertical dikes, commonly less than 1–2 m thick, with chilled margins, which bend at a distinct level and intrude parallel to the bedding of the pillow-hyaloclastite breccia to become sills with frayed edges (Figs. 1f and 12). They become thinner, fan out, and finally grade into glassy breccia. Also, small-scale finger-like buds face upwards.

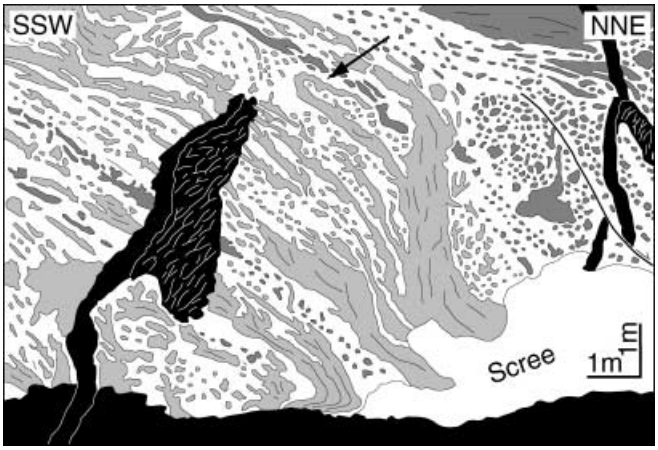

Fig. 12 Sketch of peperitic intrusive complex within basaltic lava delta (eastern coast of Porto Santo, site #3, Fig. 2). For comparison, see Fig. 8f). Intrusives are *light gray*; foreset-bedded pillow-hyaloclastite breccia is *dark-gray*; younger dikes are *black*. Note listric fault displacing dike for ca. 1 m

These dikes and sills form a peperitic intrusive complex traceable for a few tens of meters along and across strike, reaching at least 50–60 m in thickness.

The peperitic complex is closely associated with a massive, irregularly dome-shaped basaltic intrusion ca. 25–30 m thick (Fig. 1g), with protrusions into the pillow-hyaloclastite breccia. The intrusion is composed of two generations of injections. The first is dense fresh fine-grained black olivine-pyroxene-phyric basalt, and the second is weathered, light greenish-grayish aphyric, slightly vesicular basalt.

The *second generation* intrusions consist of abundant subvertical purple alkali basaltic dikes commonly less than 1 m thick which penetrate the lava delta succession. They have glassy margins and variable thickness. A few dikes are almost completely brecciated, and have multiple quench crusts and glassy breccia with jigsaw- to clast-rotated textures. The boundary with the crudely foreset-bedded pillow-hyaloclastite breccia is transitional, with an undulating zone where:

1. primary bedding of the host rock is absent, and
2. dike clasts are locally mixed with the enclosing breccia (Fig. 1h).

In this, the dike is peperitic.

Interpretation

The first generation of intrusions is interpreted as having penetrated unconsolidated water-saturated clastic rocks of the foreset-bedded lava delta succession, as indicated by completely quench-fragmented dikes and sills and irregularly-shaped domes. Emplacement must have occurred shortly after deposition of the lava delta.

The second dike generation must have been emplaced when the pillow-hyaloclastite breccia was almost lithified, because the dikes penetrate the host rock more or less regularly. Small-scale irregularities in dike orientation, however, indicate that lithification and water saturation of the country rock must have been variable. Almost completely quench-fragmented peperitic dikes must have formed where the dikes encountered water-saturated horizons with high permeabilities that became fluidized along the contacts with the dikes (Kano et al. 1993).

Later intrusions and volcanic centers (facies G)

Later intrusions were injected after the main phase of volcanic activity. Abundant picritic to rhyolitic dikes and plugs occur throughout the island. Dikes are from a few decimeters to 15 m in width and can be traced up to 1 km. Prominent plugs reach up to 250 m in diameter and can lie along feeder dikes. Voluminous intrusions form many ridge crests and peaks of Porto Santo.

A prominent dike swarm is exposed in cliffs along the central northwestern coast of Porto Santo. Dikes, accounting for approximately 60–70% of the rocks exposed, are up to 3 m thick and are hosted by massive hyaloclastite breccia. Most dikes strike north-northwest–south-southeast or northwest–southeast but orthogonal dikes striking approximately northeast–southwest also occur. The large number of dikes per unit area is interpreted as the subsurface expression of a volcanic rift zone.

Discussion of constructive and destructive processes

The lower lapilli cone apron (LLCA) originated from cone-building phreatomagmatic explosive eruptions ejecting basaltic tephra through submarine to temporarily subaerial eruption columns into the water in a submarine depositional setting (Fig. 13a). Gravitational instabilities during upward growth of the cone initiated slides and redeposition of the clastic material by gravity-driven mass flows, as indicated by abundant admixed shallow-water fossils. Most of the LLCA deposits resulted from redeposition, with only minor in-situ deposits preserved. Periods of volcanic quiescence are marked by fossiliferous horizons; most abundant are resedimented calcareous horizons rich in rhodoliths. The LLCA might have been temporarily emergent, and must have at least grown close to the water surface, as indicated by a conglomerate horizon composed of well-rounded sideromelane granules and small pebbles (Fig. 13b). The few crystalline subangular to subrounded basalt granules and oxidized lapilli might indicate emergence and a shift from explosive phreatomagmatic to pyroclastic fragmentation and quiet effusive activity, presumably when influx of external water to the vent was prevented. Thus the conglomerate, formed by wave action, might represent the erosional products of an ephemeral island. This horizon represents a period of marine wave erosion punctuating volcanic activity when the unconsolidated edifice, either emergent or very shallow submarine, was leveled to a shallow marine abrasion platform. During and after truncation of the submarine to emergent basaltic seamount, the edifice must have subsided significantly, because the overlying ULCA was also formed in shallow water, as indicated by the volcaniclastic facies and by intercalated bioclastic sandstones and the single rhodolith-coral patch

Fig. 13a–h A model for a shoaling to emergent seamount. *WB*: wavebase. Dikes are black. Deposits of the latter cartoon are *shaded*. **a** Formation of basaltic submarine to subaerial lower lapilli cone (*1*) by phreatomagmatic eruptions. Eruption column might have breached the water surface (*2*). Water-settled debris was emplaced by particle-rich mass flows (*3*). Note satellite cone on the flank (*4*). Oversteepened flanks are affected by slumps (*5*). **b** Truncation of the edifice by wave erosion. Shallow submarine platform covered by conglomerates (*1*) becomes populated by coralline algae (*2*) and algal nodules (rhodoliths) (*3*). *White arrows* indicate subsidence. **c** Formation of the submarine mugearitic to benmoreitic upper lapilli cone starts with phreatomagmatic vent-widening eruptions (*1*). Water-settled tephra emplaced by particle-rich mass flows (*2*). Unstable flanks are affected by slides (*3*). **d** Upper lapilli cone accentuated by submarine shattering of extrusive domes (*1*). Frequent dome explosions might have formed a dome-top tuff cone (*2*). Ocean currents generated erosional channel subsequently filled by glassy debris of quench-fragmented and explosively shattered trachytic dome (*3*). Periods of ceased volcanic activity represented by rhodolith-rich beds (*4*). **e** Emergent dome formed a rocky island (*1*) with beach boulder horizons along the coast (*2*). Collapse of unstable dome flanks produced a coarse-grained dense breccia deposited subaqueously (*3*). Patch reefs formed during periods of volcanic quiescence (*4*). **f** Degradation above wave base produced conglomerates (*1*). Submarine effusive activity formed a basaltic pillow – sheet flow – breccia cone (*2*). **g** Subaerial basaltic volcano (*1*) built on top of the dome. Lava flows entered the sea and formed massive lava deltas where emplaced in shallow water on flat ground (*2*) or "normal" lava-hyaloclastite breccia deltas (*3*) when encountering deep water and steep submarine slopes. Hyaloclastite breccia prism grows by foreset-bedding, intrusions (*4*), and shallow submarine basaltic flank eruptions (*5*). Fallout (*6*) was emplaced and reworked below sea level (not illustrated). **h** Ongoing effusive eruptions (*1*) were punctuated by wave erosion which produced boulder horizons (*2*). Abundant fossiliferous horizons and eroded products of the lapilli cone aprons intercalated with the lava-hyaloclastite breccia delta are not illustrated. Minor littoral cones (*3*) were produced along actively growing lava-hyaloclastite breccia deltas. Collapse of island flank represented by subaerially emplaced debris avalanche (*4*) ▶

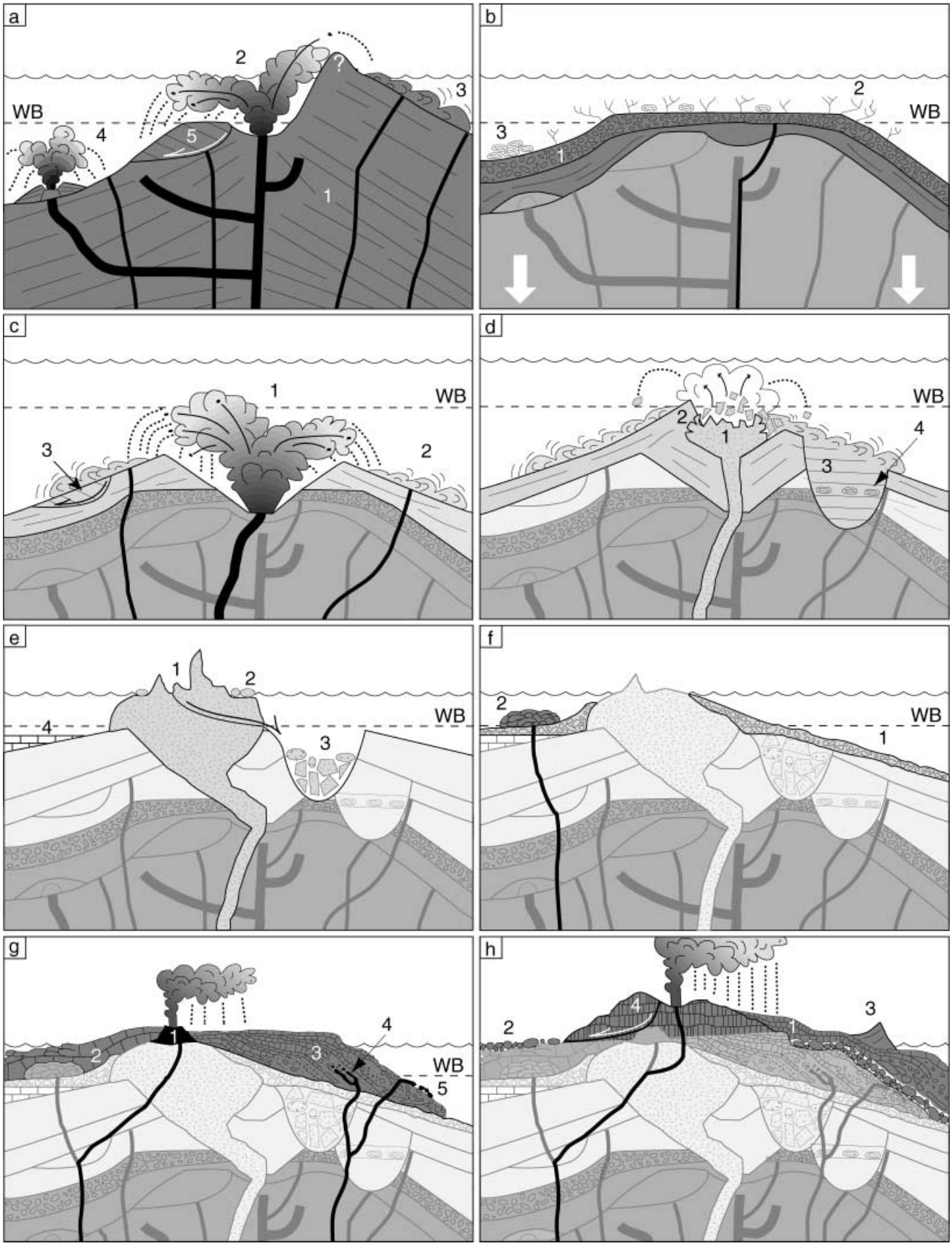
a
2
?
3
WB
4
5
1
b
2
WB
3
1
c
1
WB
3
2
d
WB
2
1
2
4
3
e
1
2
WB
4
3
f
2
WB
1
g
1
2
3
4
WB
5
h
4
3
2
1

reef which is located ca. 100 m above the conglomerate horizon. Revival of volcanic activity was characterized by episodic phreatomagmatic explosions, deposition of water-settled tephra, and subsequent resedimentation of the hydroclastic debris (Fig. 13c). Some beds enriched in non- to incipiently vesicular glassy and crystallized lapilli indicate that dome material might have contributed significantly to the growth of the cone. Periods of volcanic quiescence are represented by lenses of resedimented rhodoliths and the rhodolith-coral patch reef mentioned above. Growth of the cone near or temporarily above the water surface is indicated by conglomerates of moderately vesicular pumice in the uppermost portion of the cone. Roughly at the same time, rising trachytic magma must have caused updoming of the eastern cone flank. The changed submarine topography caused reorganization of the local ocean currents, which led to the formation of a prominent submarine channel between the updomed material and the major cone flank (Fig. 13d). The rising dome finally breached the seafloor. Quench fragmentation led to the formation of marginal in-situ hyaloclastite breccia grading into resedimentated hyaloclastites infilling the channel. Small-scale collapse of the dome initiated pyroclastic fragmentation represented by the crystal-rich volcaniclastic sandstone. Combined quench fragmentation and phreatomagmatic and pyroclastic explosions might have formed a dome-top tuff cone similar to that described from the Devonian Bunga Beds, Australia (Cas et al. 1990). Periods in which dome growth ceased are represented by:

1. trace fossils including burrows and grazing traces (Pascichnia), on surfaces of ash-rich deposits, and
2. lenses and laterally continuous beds of closely packed rhodoliths.

Degradation of the trachyte dome formed a massive coarse-grained breccia that filled a small gully crosscutting the older channel (Fig. 13e). The monomict, clast-supported breccia consists of crystalline, almost angular, trachytic dome fragments reaching up to 2 m in length; some represent column fragments. A few subrounded to rounded trachyte boulders are scattered within the breccia, probably indicating significant wave abrasion in the surf zone. Thus, prolonged volcanic activity must have built up the dome above the water surface to produce a small rocky island (Fig. 13e) comparable with the island-forming dome extrusions during the 1952–53 Myojinsho eruptions (Fiske et al. 1998).

Both LLCA and ULCA, and the relict dome-top tuff cone, are penetrated by abundant syn-volcanic dikes which dominantly strike northwest–southeast, parallel to a rift zone inferred from the bathymetric map (Fig. 1b). These syn-volcanic dikes and intrusions significantly contributed to the stabilization of the clastic aprons of the shallow-water to emergent stage, making the edifice more resistant to wave erosion.

The top of the mugearitic to trachytic succession is marked by conglomerate horizons comprising dominantly moderately to highly vesicular pumice granules and pebbles (Fig. 13f). The dominance of highly vesicular glassy clasts in the deposit – compared with the underlying deposits – suggests ongoing explosive volcanism and/or gravitational collapse of pumiceous dome material. The rounding of particles indicates subsequent reworking of the deposits in the surf zone. Degradation was concurrent with growth of small pillow-sheet flow-breccia cones of basalt (Fig. 13f). The onset of subaerial basaltic effusive activity most probably occurred atop the rocky felsic island, although direct field evidence is lacking. The products of the transition in fragmentation style from hydrovolcanic to pyroclastic-effusive are lacking on Porto Santo.

Lava flows that entered the sea created new land by shoreline progradation (Fig. 13g). This is the first order lateral and vertical growth process of volcanic ocean islands (Peterson 1976). The facies architecture of the resulting lava delta sequences reflects offshore slope angle, water depth, and lava supply rate (Schmincke et al. 1997). Steep offshore slopes and moderate lava supply rates resulted in highly fragmented hydroclastic debris with intercalated lava flow facies. This facies association, exemplified by the eastern part of Porto Santo, is typically foreset-bedded and wedge-shaped, thickening seaward. Shoreline progradation occurred by seaward-advance of bipartite lava deltas composed of steeply inclined hydroclastic prisms that filled up the submarine topography and were capped by subhorizontal submarine to subaerial lava flows. Along the eastern coast of Porto Santo (site #3, Fig. 2) voluminous syn-volcanic intrusive complexes contributed significantly to the growth of the lava delta. Peperitic intrusive complexes might be commonly overlooked, because the particle shapes of the resulting hydroclastic breccia are similar to those of the host rocks. Thus, the proportion of intrusions, that contributes to the growth of lava deltas, might generally be underestimated. In the case of Porto Santo, syn-volcanic intrusions seem to have stabilized the loose hydroclastic prism.

The entrance of lava flows into the sea may have resulted in explosive volcanic activity in the littoral environment (Mattox and Mangan 1997). Basaltic spatter and fluidal sideromelane and tachylite ash, and broken crystals, mixed and intercalated with pillow-hyaloclastite breccia indicate the formation of littoral cones at the leading edge of actively growing lava deltas. About half of the fragmented material of a littoral cone fell into the sea, represented by the clasts described, leaving a half-cone on land (Fisher and Schmincke 1984); none of the onland half-cones is preserved at Porto Santo.

Degradation of the edifice, especially during periods of volcanic inactivity, is represented by:

1. monomict conglomerates composed of subangular to well-rounded granules and pebbles of glassy and crystalline basalt;
2. conglomerates of pumiceous felsic (ULCA) and basaltic (LLCA) hyaloclastites;
3. massive, very coarse-grained epiclastic debris flow deposits; and
4. massive boulder horizons.

Colonization by marine biota occurred during these periods.

Monomict basaltic conglomerates and massive beach boulder horizons were produced by wave erosion of the earlier emplaced lava delta units. The deposits commonly have a bioclastic sandstone matrix. Gravitational instabilities of accumulated bioclastic debris led to redeposition on steep offshore slopes to produce up to 5 m thick conformable lenses between foreset units. Flat-lying insitu fossiliferous deposits are rare, represented only by a single massive bed composed of closely packed rhodoliths up to 10 cm in diameter exposed at the northwestern tip of Ilhéu de Cima (Fig. 2, inset).

Wave erosion formed submarine cliffs which subsequently became covered with thin algal mats and minor solitary corals. Epiclastic debris flows are massive, matrix- to clast supported, and consist of angular to rounded crystalline and glassy basalt blocks up to 2 m in diameter, fossiliferous debris such as coral-, rhodolith-, and bivalve fragments, and blocks of basaltic hyaloclastite breccia. The matrix is dominated by bioclastic sandstone, but admixtures of basaltic hyaloclastite and hyaloclastite breccia are common. The epiclastic debris flow deposit is interpreted as the product of a major collapse. Because the deposit lacks thermally oxidized fragments, it must have originated from failure of submarine slopes similar to those of actively growing lava deltas on Hawaii (Moore et al. 1973). Intercalated conglomerates of felsic and basaltic pumiceous conglomerates indicate simultaneous erosion of the preexisting lapilli cone aprons.

The foreset-bedded lava delta succession of eastern Porto Santo was, surprisingly, virtually unaffected by large-scale mass wasting. Collapse of the unconsolidated pillow-hyaloclastite delta might have been limited, because eruptive periods were short-lived. Such intermittent and small-volume eruptions are supported by abundant fossiliferous intercalations. Fossils include binding organisms such as encrusting red algae, which stabilized the substrate. Stabilization of the flank seems to have been assisted by few, intersecting syn-volcanic dike generations forming a grid, that intersects the pillow-hyaloclastite delta. The concept of stabilization of volcanic flanks by dike intrusion was recently introduced for the submarine flanks of Kilauea volcano (Delaney and Denlinger 1999).

The process of shoreline progradation along the western coast of Porto Santo differed fundamentally from that of its eastern counterpart (Fig. 13 g). Subhorizontal, thick tabular lava flows and associated pillow packages advanced seaward with intercalations of hyaloclastite breccia being subordinate. Crossing the shoreline, lava flows retained their coherence, which implies high lava supply rates and gentle submarine slopes. Decreasing magma supply rate resulted in transformation from tabular flows to pillow flows, a relationship well known from seamount- and mid ocean ridge studies (Ballard and Moore 1977). The lava delta succession of western Porto Santo forms a single massive structural unit which is very stable, inhibiting collapse and major redeposition. Termination of volcanic activity is represented by thin algal mats on lava flow surfaces. Aggradation was counteracted by wave erosion that produced massive boulder horizons (Figs. 11 and 13h).

Subaerial volcanic aggradation is represented by abundant lava flows and by associated scoriaceous breccia fed from numerous scoria cones scattered throughout the island (Fig. 13h). Strombolian and hawaiian fallout deposits played only a minor role in vertical and lateral accretion of the island judging from present outcrops. Flank collapse of large parts of the subaerial edifice produced a chaotic megabreccia (facies H) patchily distributed in northeastern Porto Santo. It is non-stratified and matrix-dominated, with clast size ranging from 1 mm to several meters. Clasts consist exclusively of subaerially formed basaltic rocks, and are internally fractured and sheared to produce a jigsaw puzzle texture. These criteria are consistent with basal parts of a debris avalanche deposit (Ui et al. 2000) post-dating the last subaerial volcanic activity on Porto Santo.

Water depth of eruptions and deposition

The water depth at which submarine volcanic rocks were erupted and deposited can be estimated using a variety of data including: fossils, conglomerates, vesicularity of juvenile particles, and volatile content of fresh volcanic glass (Fisher and Schmincke 1984).

The vesicularity of juvenile particles of both LLCA and ULCA crudely increases toward the top of each deposit. Two shoaling cycles can be inferred from the presence of conglomerates on top of LLCA and ULCA. The conglomerates capping ULCA must have formed in a shoreline environment at water depths of no more than a few tens of meters well above the fair weather wavebase. Sulfur content of sideromelane particles from the LLCA conglomerate ranges from 200 to 600 ppm (Schmidt 2000), indicating shallow water to subaerial eruptions (Moore and Clague 1992) with significant degassing before quenching. Coralline algal nodules (rhodoliths) form lenses embedded in the hyaloclastites. Most rhodoliths are spherical and compact in shape, with thin (<1 cm) concentric algal coatings surrounding lapilli-sized volcanic clasts. Living beds of such nodular aggregates of coralline algae have been observed from the lowest intertidal zone to depths of 268 m (Bosellini and Ginsburg 1971; Littler et al. 1991). Here, the simple growth pattern and compact shape indicate exposure to a high-energy regime that causes frequent movement, because of wave action or strong ocean currents (Manker and Carter 1987; Braga and Martin 1988). Hermatypic corals are the main constituent of the small patch reef embedded in the ULCA, and indicate growth within the photic zone. The most favorable water depth for the growth of corals is less than 20 m, but can be as deep as 70 m if water is clear (James 1984).

In summary, both lapilli cone successions formed in shallow water most likely between ca. 100 and 0 m water depth.

Juvenile glassy clasts of the basaltic lava delta succession are mostly non-vesicular and crowded with plagioclase microlites, together indicating extensive degassing and crystallization during subaerial flowage before quenching on contact with seawater (Moore 1975; Moore and Clague 1987). Extensive degassing is further supported by samples which have sulfur contents below the detection limit (<125 ppm; unpublished data). In contrast, a few samples have sulfur contents between 250 and 320 ppm (Schmidt unpublished data) which might indicate very shallow submarine eruptions (Moore and Clague 1992). Bioclastic sandstones embedded in the basaltic lava delta succession contain fragments of coralline red algae, corals, thick-shelled bivalves, echinoid plates and spines. This faunal community clearly indicates a very shallow water- and high energy setting. Thin algal mats, which form the substrate for solitary corals atop submarine cliffs, further support high wave energy along a rocky shoreline; such a shoreline is also indicated by prominent boulder horizons.

In summary, the lava delta succession originated from subaerial lava flows that entered the sea, perhaps accompanied by minor shallow submarine eruptions along the east coast of Porto Santo. Associated faunal communities confirm intertidal to sublittoral environments.

Conclusions

1. During shoaling and emergence of the shallow water seamount of Porto Santo, numerous dynamic processes contributed to growth and stabilization of the edifice. These processes include submarine and subaerial phreatomagmatic and pyroclastic explosions, submarine explosive shattering, and quench fragmentation of extrusive domes, as well as submarine and subaerial effusive activity.
2. Submarine erupted tephra was frequently redeposited by particle-rich mass flows forming gently dipping lapilli cone aprons, in situ deposits represented by the satellite cone (facies A-2, LLCA) being subordinate. The clastic edifice became stabilized by abundant syn-volcanic dikes and voluminous intrusions.
3. All volcanic rocks of the submarine stratigraphic section exposed were erupted and deposited in water depths ranging from 0 to <250 m and thus represent only the uppermost part of its submarine evolution.
4. Constructional volcanic activity was frequently counteracted by degradation owing to the gravitational instability of the edifice and by wave action and ocean currents during periods of volcanic quiescence.
5. Island-forming eruptions deposited tephra to form an emergent lapilli cone, which was subsequently eroded by wave action and ocean currents (LLCA). Dome extrusion also occurred, possibly associated with a dome-top tuff cone originating from explosive shattering of dome material.
6. The facies architecture of basaltic lava-hyaloclastite deltas basically depends on lava supply rate, lava viscosity, offshore slope angle, and wave energy. Pahoehoe lava flows with moderate supply rates that encounter steep offshore slopes along a high-energy shoreline form “normal” lava deltas composed of a lower structural unit of strongly fragmented, foreset-bedded hydroclastic rocks, and an upper unit of submarine to subaerial lava flows. During growth of hydroclastic prisms resedimentation by means of monomict debris flow deposits is a common process. Large scale failure of submarine slopes was rare.

Prolonged supply rates, together with subhorizontal offshore slope along a low-energy coast led to tabular lava flows which remained coherent when crossing the shore line. Decreasing lava supply rates resulted in the dominance of pillowed flows. Slope failure and redeposition processes must have been almost absent since the succession was very stable. The resulting lava delta is composed of only one, massive, structural unit and, in this, significantly contrasts with “normal” lava deltas.

7. The hydroclastic prism of the lava-hyaloclastite breccia delta grew dominantly by accretion of foreset-beds but also by complex syn-volcanic intrusions. In the case of Porto Santo, numerous generations of intersecting syn-volcanic dikes and plugs stabilized the volcanic flank.

Acknowledgements We acknowledge Miguel Moreins (Assisténcia Naútica, LDA., Porto Santo), Geoff Rees, and Barbara Burns and Thomas Schmidt who kindly facilitated trips around Porto Santo by boat to study the cliff sections. We also thank Domingos Rodrigues (Madeira University) for logistic support and discussions in the field. Many thanks to Wolf-Christian Dullo for determining benthic foraminifers. Discussions with Jocelyn McPhie are gratefully acknowledged. This paper forms part of the requirement for the Ph.D. of RS. Our study was financed by the Deutsche Forschungsgemeinschaft (grant Schm 250/49) and the Land Schleswig-Holstein. We thank James White, Andreas Klügel, and Rodey Batiza for their critical reviews and comments, which substantially improved the manuscript.

References

Ballard RD, Moore JG (1977) Photographic atlas of the Mid-Atlantic Ridge rift valley. Springer, Berlin Heidelberg New York, pp 1–114

Batiza R, White JDL (2000) Submarine lavas and hyaloclastite. In: Sigurdsson H (ed) Encyclopedia of volcanoes. Academic Press, San Diego, pp 361–381

Bosellini A, Ginsburg R (1971) Form and internal structure of recent algal nodules (rhodolites) from Bermuda. J Geol 79:669–682

Braga JC, Martin JM (1988) Neogene coralline-algal growth-forms and their palaeoenvironments in the Almanzora river valley (Almeria, SE Spain). Palaeogeogr Palaeoclim Palaeoecol 67:285–303

Cas RAF, Allen RL, Bull SW, Clifford BA, Wright JV (1990) Subaqueous, rhyolitic dome-top tuff cones: a model based in the Devonian Bunga beds, southeastern Australia and a modern analogue. Bull Volcanol 52:159–174

Cas RAF, Landis CA, Fordyce RE (1989) A monogenetic, surtla-type, surtseyan volcano from the Eocene-Oligocene Waiareka-Debdorah volcanics, Otago, New Zealand: a model. Bull Volcanol 51:281–298

Clague DA, Davis AS, Bischoff JL, Dixon JE, Geyer R (2000) Lava bubble-wall fragments formed by submarine hydrovolcanic explosions on Loihi seamount and Kilauea volcano. Bull Volcanol 61:437–449

Delaney PT, Denlinger RP (1999) Stabilization of volcanic flanks by dike intrusion: an example from Kilauea. Bull Volcanol 61:356–362

Feraud G, Schmincke H-U, Lietz J, Gastaud J, Pitchard G, Bleil U (1981) New K-Ar ages, chemical analyses and magnetic data of rocks from the islands of Santa Maria (Azores), Porto Santo and Madeira (Madeira Archipelago) and Gran Canaria (Canary Islands). Bull Volcanol 44:359–375

Fink JH, Anderson SW (2000) Lava domes and coulees. In: Sigurdsson H (ed) Encyclopedia of volcanoes. Academic Press, San Diego, pp 307–319

Fink JH, Manley CR (1989) Explosive volcanic activity generated from within advancing silicic lava flows. In: Latter JH (ed) Volcanic hazards. IAVCEI Proc Volcanol 1. Springer, Berlin Heidelberg New York, pp 169–179

Fisher RV (1968) Puu Hou littoral cones, Hawaii. Geol Rundsch 57:837–864

Fisher RV, Schmincke H-U (1984) Pyroclastic rocks. Springer, Berlin Heidelberg New York, pp 1–472

Fiske RS, Cashman KV, Shibata A, Watanabe K (1998) Tephra dispersal from Myojinsho, Japan, during its shallow submarine eruption of 1952–1953. Bull Volcanol 59:262–275

Fleet AJ, McKelvey BC (1978) Eocene explosive submarine volcanism, Ninetyeast Ridge, Indian Ocean. Mar Geol 26:73–97

Fornari DJ, Ryan WBF, Fox PJ (1984) The evolution of craters and calderas on young seamounts: insights from Sea Marc I and Sea Beam Sonar surveys of a small seamount group near the axis of the East Pacific Rise at ~10°N. J Geophys Res 89:11069–11083

Francis P (1995) Fire and water. Geology Today 11:27–31

Furnes H, Fridleifsson IB, Atkins FB (1980) Subglacial volcanics – on the formation of acid hyaloclastites. J Volcanol Geotherm Res 8:95–110

Geldmacher J, Bogaard PVD, Hoernle K, Schmincke H-U (2000) 40Ar/39Ar age dating of the Madeira Archipelago and hotspot track (eastern North Atlantic). G3 Geochem Geophys Geosyst 1

Gill J, Horssander P, Lapierre H, Taylor R, Kaiho K, Koyama M, Kusakabe M, Aitchison J, Cisowski S, Dadey K, Fujioka K, Klaus A, Lovell M, Marsaglia K, Pezard P, Taylor B, Tazaki K (1990) Explosive deep water basalt in the Sumisu backarc rift. Science 248:1214–1217

Houghton BF, Wilson CJN (1989) A vesicularity index for pyroclastic deposits. Bull Volcanol 51:451–462

James NP (1984) Reefs. In: Walker RG (ed) Facies models. Geol Assoc Canada, Toronto, pp 229–244

Jones JG (1969) Pillow lavas as depth indicators. Am J Sci 267:181–195

Jones JG, Nelson PHH (1970) The flow of basalt lava from air into water – its structural expression and stratigraphic significance. Geol Mag 107:13–19

Kano K, Yamamoto T, Takeuchi K (1993) A Miocene island-arc volcanic seamount: the Takashibiyama formation, Shimane Peninsula, SW Japan. J Volcanol Geotherm Res 59:101–119

Kano K, Yamamoto T, Ono K (1996) Subaqueous eruption and emplacement of the Shinjima pumice, Shinjima (Moeshima) Island, Kagoshima Bay, SW Japan. J Volcanol Geotherm Res 71:187–206

Kokelaar BP (1983) The mechanism of surtseyan volcanism. J Geol Soc Lond 140:939–944

Kokelaar BP (1986) Magma-water interactions in subaqueous and emergent basaltic volcanism. Bull Volcanol 48:275–289

Lietz J, Schwarzbach M (1970) Neue Fundstellen von marinem Tertiär auf der Atlantik-Insel Porto Santo (Madeira-Archipel). Neues Jahrb Geol Palaeontol Monatsh 5:270–282

Littler M, Littler D, Hanisak M (1991) Deep-water rhodolith distribution, productivity, and growth history at sites of formation and subsequent degradation. J Exp Mar Biol Ecol 150:163–182

Lonsdale P, Batiza R (1980) Hyaloclastite and lava flows on young Pacific seamounts examined with a submersible. Geol Soc Am Bull 91:545–554

Macedo CR, Costa V, Ferreira M (1974) K/Ar ages on the central Atlantic islands. Int Meet Geochronol Cosmochronol Isotope Geol. Paris

Manker JP, Carter BD (1987) Paleoecology and paleogeography of an extensive rhodolith facies from the Lower Oligocene of South Georgia and North Florida. Palaios 2:181–188

Mattox TN, Mangan MT (1997) Littoral hydrovolcanic explosions: a case study of lava-seawater interaction at Kilauea Volcano. J Volcanol Geotherm Res 75:1–17

McPhie J (1995) A Pliocene shoaling basaltic seamount: Ba volcanic group at Rakiraki, Fiji. J Volcanol Geotherm Res 64:193–210

McPhie J, Hunns SR (1995) Secondary welding of submarine, pumice-lithic breccia at Mount Chalmers, Queensland, Australia. Bull Volcanol 57:170–178

Moore JG (1970) Pillow lava in a historic lava flow from Hualalai Volcano, Hawaii. J Geol 78:239–242

Moore JG (1975) Mechanism of formation of pillow lava. Am Sci 63:269–277

Moore JG (1985) Structure and eruptive mechanisms at Surtsey Volcano, Iceland. Geol Mag 122:649–661

Moore JG, Clague D (1987) Coastal lava flows from Mauna Loa and Hualalai volcanoes, Kona, Hawaii. Bull Volcanol 49:752–764

Moore JG, Clague DA (1992) Volcano growth and evolution of the island of Hawaii. Geol Soc Am Bull 104:1471–1484

Moore JG, Fiske RS (1969) Volcanic substructure inferred from dredge samples and ocean-bottom photographs, Hawaii. Geol Soc Am Bull 80:1191–1202

Moore JG, Phillips RL, Grigg RW, Peterson DW, Swanson DA (1973) Flow of lava into the sea, 1969–1971, Kilauea Volcano, Hawaii. Geol Soc Am Bull 84:537–546

Peterson DW (1976) Processes of volcanic island growth, Kilauea volcano, Hawaii. In: Ferran O (ed) Andean and Antarctic volcanology problems. IAVCEI, Santiago, Chile, pp 172–189

Porebski SJ, Gradzinski R (1990) Lava-fed Gilbert-type delta in the Polonez Cove formation (Lower Oligocene), King George Island, West Antarctica. In: Colella A, Prior DB (eds) Coarse-grained deltas. Int Assoc Sediment, Spec Pub 10. Blackwell, Oxford, pp 335–351

Poulet Scrope G (1862) Volcanoes: fire from the earth. Longman, London, pp 1–490

Rodrigues DMM, Cachao M, Da Silva CM (1998) New biostratigraphic data (calcareous nanofossils) from fossiliferous levels of the Miocene volcanic island of Porto Santo (Madeira, Portugal). Abs, IAVCEI, Magmatic diversity: volcanoes and their roots. Cape Town

Schmidt R (2000) From seamount to oceanic island, Porto Santo, Madeira Archipelago (central East-Atlantic). PhD Thesis, Christian Albrechts University Kiel, pp 1–171

Schmidt R, Schmincke H-U (2000) Seamounts and island building. In: Sigurdsson H (ed) Encyclopedia of volcanoes. Academic Press, San Diego, pp 383–402

Schmincke H-U (1967) Fused tuff and peperites in south-central Washington. Geol Soc Am Bull 78:319–330

Schmincke H-U, Weibel M (1972) Chemical study of rocks from Madeira, Porto Santo, and São Miguel, Terceira (Azores). Neues Jahrb Mineral Abh 117:253–281

Schmincke H-U, Staudigel H (1976) Pillow lavas on central and eastern Atlantic islands (La Palma, Gran Canaria, Porto Santo, Santa Maria). (Preliminary report). Bull Soc Géol Fr 7:871–883

Schmincke H-U, Bednarz U (1990) Pillow, sheet flow and breccia flow volcanoes and volcano-tectonic hydrothermal cycles in the extrusive series of the northeastern Troodos ophiolite (Cyprus). In: Malpas J et al. (eds) Ophiolites: oceanic crustal analogues. Geological Survey of Cyprus, Nicosia, pp 185–206

Schmincke H-U, Behncke B, Grasso M, Raffi S (1997) Evolution of the northwestern Iblean Mountains, Sicily: uplift, Pliocene/Pleistocene sea-level-changes, paleoenvironment, and volcanism. Geol Rundsch 86:637–669

Scutter CR, Cas RAF, Moore CL, de Rita D (1998) Facies architecture and origin of a submarine rhyolitic lava flow-dome complex, Ponza, Italy. J Geophys Res 103:27551–27566

Smellie JL, Hole MJ (1997) Products and processes in Pliocene-Recent, subaqueous to emergent volcanism in the Antarctic peninsula: examples of englacial surtseyan volcano construction. Bull Volcanol 58:628–646

Smith JV, Yamauchi S, Miyake Y (1993) Microshear zones in a Miocene submarine dacite dome of southwest Japan. Bull Volcanol 55:438–442

Smith TL, Batiza R (1989) New field and laboratory evidence for the origin of hyaloclastite flows on seamount summits. Bull Volcanol 51:96–114

Smith WHF, Sandwell DT (1997) Global sea floor topography from satellite altimetry and ship depth soundings. Science 277:1956–1962

Sohn YK (1995) Geology of Tok Island, Korea: eruptive and depositional processes of a shoaling to emergent volcano. Bull Volcanol 56:660–674

Sohn YK, Chough SK (1992) The Ilchulbong tuff cone, Cheju Island, South Korea: depositional processes and evolution of an emergent, surtseyan-type tuff cone. Sedimentology 39:523–544

Staudigel H, Schmincke H-U (1984) The Pliocene seamount series of La Palma/Canary Islands. J Geophys Res 89:11195–11215

Ui T, Takarada S, Yoshimoto M (2000) Debris avalanches. In: Sigurdsson H (ed) Encyclopedia of volcanoes. Academic Press, San Diego, pp 617–626

Vespermann D, Schmincke H-U (2000) Scoria cones and tuff rings. In: Sigurdsson H (ed) Encyclopedia of volcanoes. Academic Press, San Diego, pp 683–694

Walker GPL (1992) Morphometric study of pillow-size spectrum among pillow lavas. Bull Volcanol 54:459–474

Watts AB, ten Brink US (1989) Crustal structure, flexure, and subsidence history of the Hawaiian islands. J Geophys Res 94:10473–10500

Werner R, Schmincke H-U (1999) Englacial vs lacustrine origin of volcanic table mountains: evidence from Iceland. Bull Volcanol 60:335–354

White JDL (1996) Pre-emergent construction of a lacustrine basaltic volcano, Pahvant Butte, Utah (USA). Bull Volcanol 58:249–262

Yamagishi H, Dimroth E (1985) A comparison of Miocene and Archean rhyolite hyaloclastites: evidence for a hot and fluid rhyolite lava. J Volcanol Geotherm Res 23:337–355